

Department of Physics and Astronomy  
University of Heidelberg

**Bachelor Thesis**

in Physics

submitted by

**Denis Alevi**

born in Berlin, Germany

**March 2015**



# Investigating Competitive Dynamics in a Recurrent Neural Network on Neuromorphic Hardware

**This Bachelor Thesis has been carried out by Denis Alevi at the**

**KIRCHHOFF INSTITUTE FOR PHYSICS**

**RUPRECHT-KARLS-UNIVERSITÄT HEIDELBERG**

**under the supervision of**

**Prof. Dr. Karlheinz Meier**



## **Investigating Competitive Dynamics in a Recurrent Neural Network on Neuromorphic Hardware**

A recurrent neural network is implemented on neuromorphic hardware and investigated for its competitive dynamics. Emulation experiments on the High Input Count Analog Neural Network (HICANN) chip are conducted through the high level PyNN frontend, giving easy access to the complex hardware.

In a first step, the parameters available after calibration are characterized for their influence on firing rates of hardware neurons. A blacklisting method is developed to mark neurons not responding to a given external stimulus.

The neural network is then emulated step by step, investigating the firing rates of competing populations for different stimuli. Measurement results are compared with simulations using the Executable System Specification (ESS).

Similar network behaviour in ESS simulation and hardware emulation can be obtained and possible techniques for improving the experiment results are discussed.

## **Untersuchung von Kompetitiver Dynamik in einem Rekurrenten Neuronalen Netz auf Neuromorpher Hardware**

Ein rekurrentes neuronales Netz wird auf neuromorpher Hardware implementiert und hinsichtlich seiner konkurrierenden Feuerrateneigenschaften untersucht. Über die Abstraktionsebene der Softwareschnittstelle PyNN werden Experimente auf der komplexen Hardware durchgeführt.

Zunächst werden die verfügbaren Parameter auf ihren Einfluss auf die Feuerraten der Hardwareneurone hin überprüft. Eine Methode zur Selektion von Neuronen mit dem gewünschten Verhalten wird implementiert.

Das neuronale Netz wird daraufhin Schritt für Schritt emuliert, wobei die Feuerraten konkurrierender Neuronenpopulationen für verschiedene Stimuli untersucht werden. Ergebnisse der Hardwareexperimente werden mit denen aus Softwaresimulationen mit der Executable System Specification (ESS) verglichen.

Es wird vergleichbares Netzwerkverhalten in der ESS-Simulation und Hardwareemulation erreicht. Mögliche Verbesserungen werden diskutiert.



# Contents

<b>1</b>	<b>Introduction</b>	<b>1</b>
1.1	Neuromorphic Hardware . . . . .	1
1.2	Software Framework . . . . .	1
1.3	Executable System Specification (ESS) . . . . .	2
<b>2</b>	<b>Towards uniform spiking rates</b>	<b>3</b>
2.1	Characterization of available parameter space . . . . .	5
2.1.1	Calibration settings . . . . .	5
	Reversal potentials . . . . .	6
	Resting potential and membrane time constant . . . . .	6
	Synaptic time constants . . . . .	7
	Refractory time . . . . .	7
	Reset potential and spiking threshold . . . . .	7
	Adaption and exponential term . . . . .	7
	Synaptic weights . . . . .	8
	Synaptic delays . . . . .	8
	Synaptic plasticity . . . . .	8
2.2	Blacklisting . . . . .	8
2.2.1	Requirements . . . . .	9
	Number of neurons emulated on one HICANN chip at once . . . . .	9
	Blacklisting synapse drivers . . . . .	10
2.2.2	Method . . . . .	12
	Always spiking neurons . . . . .	12
	Not-spiking neurons . . . . .	12
2.2.3	Results . . . . .	12
2.3	Investigating rate response to parameter changes . . . . .	14
2.3.1	Inputrate . . . . .	14
2.3.2	Refractory time $\tau_{\text{refrac}}$ . . . . .	20
2.3.3	Synaptic weights . . . . .	20
2.3.4	Threshold voltage ( $V_{\text{thresh}}$ ) . . . . .	20
2.4	Summary . . . . .	20
<b>3</b>	<b>Emulating a recurrent neural network</b>	<b>25</b>
3.1	Network Topology . . . . .	25
3.2	Methods . . . . .	26
3.2.1	Choosing the neurons for each population . . . . .	26

3.2.2	ESS vs. HICANN . . . . .	26
3.2.3	Investigating different parts of the network . . . . .	27
3.2.4	Investigated network properties . . . . .	27
	Point of equal firing rates . . . . .	27
3.3	Results . . . . .	27
3.3.1	Only one population with poisson stimulus . . . . .	28
3.3.2	Two populations with only unidirectional inhibitory connections . . . . .	28
3.3.3	Emulating the entire network . . . . .	30
3.3.4	Results with correctly applied blacklisting . . . . .	30
3.3.5	Observation of network behaviour on neuron level . . . . .	30
<b>4</b>	<b>Discussion and Outlook</b>	<b>39</b>
	<b>Appendix</b>	<b>41</b>
	<b>Nomenclature</b>	<b>46</b>
	<b>Bibliography</b>	<b>49</b>



# 1 Introduction

The human brain is capable to coordinate complex motion sequences. The fine and gross motor skills are the result of interactions between multiple populations of neurons localized in different parts of the human brain. For the pathogenesis of Parkinson's disease, a widely known model is the hypothesis of degeneration of neurons in certain parts of the brain (*Cutsuridis, 2013*). As a result, the interactions between neuron populations controlling the motor skills is disturbed, leading to the well-known symptoms such as tremor or rigidity.

In order to better understand such underlying principles of interplay between neurons, network models are developed and investigated, e.g. in simulations. But the complexity of the brain, where billions of neurons are processing information through a very dense connectivity, limits the simulation possibilities when using today's Von Neumann computer architecture.

Therefore, in a different approach neuromorphic computer systems are developed. These new architectures promise to solve the computational limitations through highly parallel information processing and use very little energy compared to what supercomputers need to simulate just fractions of the human brain.

## 1.1 Neuromorphic Hardware

The central element of the neuromorphic hardware platform used in this thesis is the High Input Count Analog Neural Network (HICANN) chip, which basis elements are the correlates from biology: analog neurons and synapses. 384 of these HICANN chips, each consisting of 512 neuron circuits and several thousand possible synaptic connections, are build into one wafer module, of which several can be interconnected.

This hardware architecture allows a massively parallelized emulation of neural networks. For further information about the hardware we refer to *HBP SP9 partners (2014)* and *Schemmel et al. (2010)*.

## 1.2 Software Framework

### PyNN

For implementing neural networks, the high level frontend PyNN is used. PyNN is a description language for neuron networks implemented in Python. By choosing different backends, the same code can be executed on hardware or by using a simulator.

## 1 Introduction

### **Marocco**

*Marocco* is the software responsible for translating a neural network to the hardware representation, placing neurons and routing connections by using as less resources as possible.

### **Cake**

*Cake* is the software defining how calibration measurements are conducted.

## **1.3 Executable System Specification (ESS)**

The ESS simulates the HICANN wafer system, replicating communication infrastructure, simulating synapse loss and hardware limitations. As default ideal neurons are simulated which behave exactly the same. Additionally parameters noise can be induces, simulating hardware variations.

## 2 Towards uniform spiking rates

In many neuronal networks spiking rates for different neurons or populations are chosen as measure to characterize network behaviour. When implementing such networks on neuromorphic hardware it is important to obtain similar spiking rates for network populations or subunits of same type. But emulation experiments on the HICANN chip show neuron-to-neuron and trial-to-trial variations in both, parameter values and firing rates. One cause for spike rate variability across neurons are transistor variations. Calibration techniques are used to minimize these technical variations. Another cause for spike rate variability lies in the variations of floating gates used for storing neuron parameters (*Schmidt, 2014*).

To measure the spike rate variability across different neurons and for different parameters, the following measurement setup is used throughout this chapter:

- Multiple neurons with same parameters are placed on one HICANN chip.
- An external stimulus is created through a poisson source.
- Each emulated neuron receives the same stimulus from the same poisson source with same connection parameters.
- All spikes of each neuron are counted and divided by the simulation time to obtain the spike rates.
- The experiment is repeated multiple times with the same seed for the poisson process, i.e. the same spike train stimulus is sent for each repetition.

If not stated explicitly, measurements in this thesis are performed on the HICANN 276 of the first prototype wafer system. Hardware neuron size is set to 4 for all measurements an a speedup factor of  $10^4$  is used. The HICANN chip is operated at a clock frequency of 100 Hz and the inter spike intervals (ISIs) of the background event generators are set to 10 000 to lock the layer 1 repeaters. Neuron block 7 is not used since the output buffer is reserved for external input and background event generation. This leaves 7 neuron blocks with 64 dendritic membrane circuits (DenMems) each for experiments. Therefore,  $\frac{7 \times 64}{4} = 112$  size 4 neurons can be emulated on one HICANN. Each emulation experiment on the HICANN is run for a simulation time of 10 000 ms biological time, corresponding to 1 ms emulation time on the hardware for a speedup of  $10^4$ .

For all measurements calibration data from a previous calibration measurement is used. The calibration settings are explained in section 2.1.1.

## 2 Towards uniform spiking rates

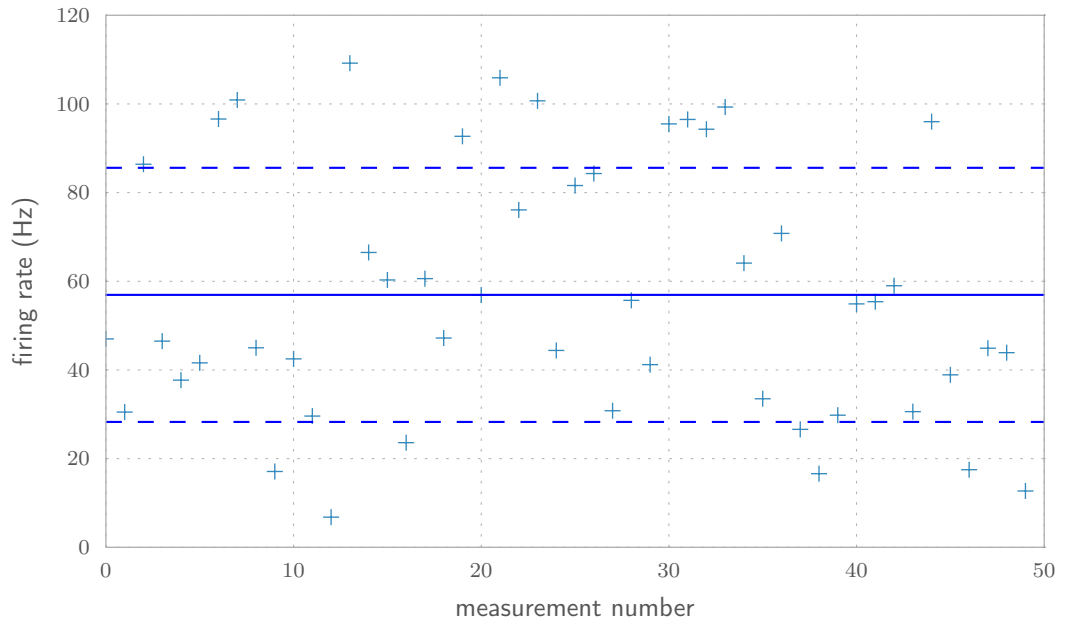


Figure 2.1: Measured rates of one hardware neuron of size 4 for 50 repetitions. The straight line marks the mean  $\mu$  and the dashed lines mark the standard deviation  $\pm\sigma$ . This is the neuron with index 12 in figure 2.2.

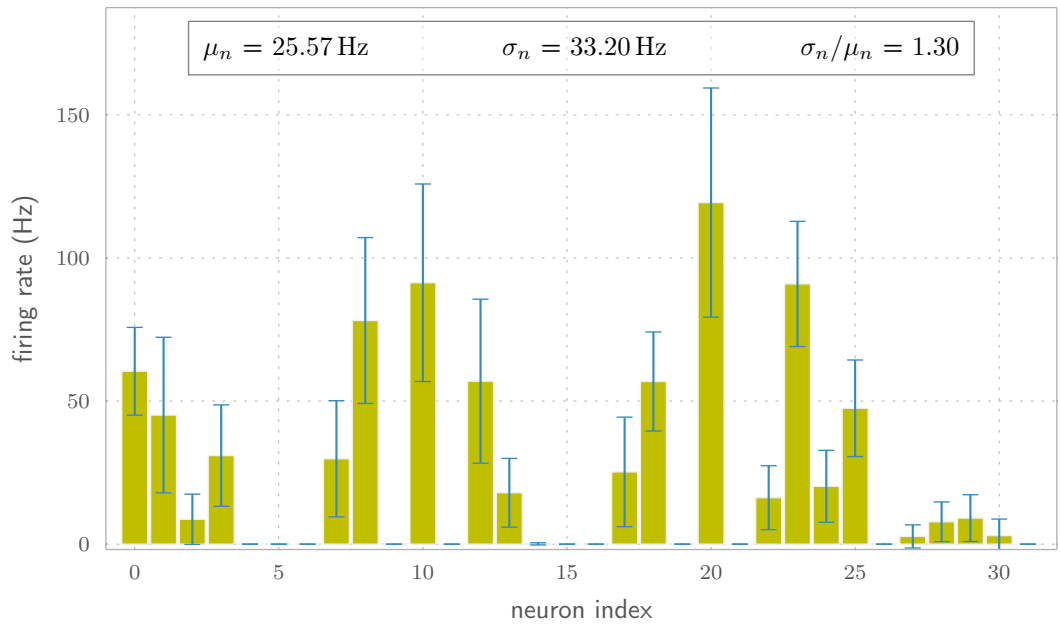


Figure 2.2: Mean and standard deviations of 50 repetitions for different hardware neurons of size 4. In each repetition all neurons are emulated parallel on the first two neuron blocks of one HICANN chip.

In figure 2.1 the trial to trial variations for one exemplary neuron are shown. As a measure of the variations the standard deviation is calculated.<sup>1</sup>

The mean firing rates and standard deviations for some exemplary neurons are shown in figure 2.2. The spiking behaviour of neurons with same parameters and same external stimulus differs significantly for emulations on different hardware neurons. This can be understood by the lack of membrane time constant and refractory period calibrations described in section 2.1.1, as well as by varying strength and time course of the synaptic input.

One target of the work in this thesis was to obtain neuron populations responding similar to external stimulus and to be able to control their spiking behaviour by changing neuron parameters. To achieve this, three steps are taken:

- Characterizing the available hardware parameters for influencing spike response. (section 2.1)
- Blacklisting neurons not responding in a desired way. (section 2.2)
- Sorting remaining neurons in multiple populations depending on their spike response.

## 2.1 Characterization of available parameter space

The parameters accessible from the PyNN interface are the neuron parameters of the used neuron model and the connection parameters describing the synapse properties.

For hardware emulations only conductance based neuron models are available. One can choose between the Adaptive Exponential Integrate and Fire (AdEx) model and the Leaky Integrate and Fire (LIF) model as described in *Brette and Gerstner (2005)*. For those neuron parameters calibration methods described by *Schmidt (2014)* were developed to reduce parameter variations on the HICANN chip.

The synapse dynamics are by default only governed by the synaptic weight and delays. Optionally synaptic plasticity mechanisms can be implemented. Both, Short Term Plasticity (STP) and Spike-Timing Dependent Plasticity (STDP) are in general supported on the HICANN chip.

### 2.1.1 Calibration settings

In the following section, a short summary of the used calibration methods is given to identify the parameters available to change neuron behaviour from PyNN with the currently available calibration. Information concerning calibration methods and parameter

---

<sup>1</sup>All standard deviations are calculated with a denominator of N-1 to account for the finite number of measurements.  $\sigma_{N-1} = \sqrt{\frac{1}{N-1} \sum_{i=1}^N (x_i - \mu)^2}$ ,

## 2 Towards uniform spiking rates

transformation are taken from *Schmidt* (2014) if not stated otherwise. In table 2.1 all biological parameters and their corresponding hardware parameters accessible from PyNN are listed and a summary of the parameter availability explained in this section is given. The effect of changing the available parameters on spiking rates of neurons is characterized in section 2.3.

Table 2.1: Summary of accessibility of biological (bio) parameters and corresponding hardware (hw) parameters for changing network behaviour from PyNN and for the current calibration state.

bio parameter	hw parameter	accessibility	comment
$c_m$		<i>marocco</i> switch	smallcap and bigcap
$\tau_m$	$I_{gl}$	fixed value	<i>cake</i> : maximize PSP
$\tau_{refrac}$	$I_{pl}$	free to choose	$I_{pl}(\text{DAC}) = \tau_{refrac}$
$\tau_{syn,E} / \tau_{syn,I}$	$V_{syntex} / V_{syntci}$	fixed value	<i>cake</i> : maximize PSP
$E_{rev,E} / E_{rev,I}$	$E_{synx} / E_{syni}$	not used	fixed distance to $E_1$
$V_{reset}^{bio}$	$V_{reset}^{hw}$	free to choose	-
$V_{rest}$	$E_1$	not used	value used in $I_{gl}$ calibration
$V_{thresh}$	$V_t$	free to choose	-
adaption		not used	calibration not implemented yet
exponential term		not used	calibration not implemented yet
<i>weight</i>	4 bit <i>weight</i>	only 16 values	no calibration available
<i>delay</i>	not a parameter	no influence	technical delays on hw
STP		not used	calibration not implemented yet

### Reversal potentials

Conductances in neurons on hardware are emulated through operational transconductance amplifiers (OTAs). Since differential voltages larger than 100 mV leave the linear range of the OTA (*Kiene*, 2014), distances between leakage potential  $E_1$  and synaptic reversal potential  $E_{syni}$  or  $E_{synx}$  above 100 mV are avoided. This corresponds to a voltage difference of 10 mV in biological domain<sup>2</sup>. The neuron to neuron variability of  $E_1$  was found to be lowest when  $E_1$  is equidistant to both,  $E_{syni}$  and  $E_{synx}$ . Therefore, for the measurements in this work the biological parameters for the reversal potential  $E_{rev,I}$  and  $E_{rev,E}$  are kept fixed at  $V_{rest} - 10$  mV and  $V_{rest} + 10$  mV, respectively. Lower distances are possible but would increase the effect of floating gate variations and decrease the total dynamic range of the membrane potential.

### Resting potential and membrane time constant

Different values of the biological membrane time constant  $\tau_m$  are realized by three mechanisms on the hardware. First  $\tau_m$  scales inversely with a leakage bias current  $I_{gl}$ . Second

<sup>2</sup>The scaling factor between biological and hardware voltages is arbitrary. The current voltage translation is  $V_{hardware} = 10 \times V_{biological} + 1200$  mV as is described in *Schmidt* (2014).

## 2.1 Characterization of available parameter space

the speedup factor of the hardware influences current mirrors which result in a scaling factor for  $I_{gl}$ . Third there are two different settings of the membrane capacitance available on the HICANN chip, called bigcap and lowcap setting. In the current software stage the biological membrane capacitance parameter  $c_m$  does not change the capacitance on the hardware. Instead the hardware capacitance can be switched manually through *marocco* and is by default set to bigcap. This setting is not changed throughout this thesis.

The available calibration framework used in this thesis calibrates  $I_{gl}$  towards a maximal effect on the postsynaptic potential (PSP). For lower values of  $I_{gl}$  the leakage conductance decreases resulting in higher PSPs but this can affect the resting potential  $V_{rest}$  due to leakage currents from the synaptic input circuit. The calibration searches for the lowest value of  $I_{gl}$  while not losing control over the resting potential  $V_{rest}$ . This is done by choosing a fixed  $V_{rest}$  prior to the calibration to make sure it can still be reached for a chosen  $I_{gl}$  value. The chosen  $I_{gl}$  value is then fixed and the  $\tau_m$  set in PyNN is ignored. When using this calibration, changing  $V_{rest}$  to a value other than used for the calibration method can result in uncharacterized behaviour. Therefore, the biological parameters  $V_{rest}$  can not reliably be used for changing neuron dynamics.

### Synaptic time constants

The synaptic time constants  $\tau_{syn,I}$  and  $\tau_{syn,E}$  are controlled by the floating gate values  $V_{syntci}$  and  $V_{syntcx}$ , respectively. The calibration software searches again for maximal effect of PSPs and sets the hardware parameters to fixed values, not influenced by the chosen biological parameters.

### Refractory time

The refractory period  $\tau_{refrac}$  determines the hardware parameter  $I_{pl}$ . For measurements in this thesis, an  $I_{pl}$  calibration was not available. To have controlled influence on the  $I_{pl}$  parameter, the transformation of biological to hardware parameter was disabled. Instead the value for  $\tau_{refrac}$  defined in PyNN is passed directly as digital to analog converted (DAC) value to the hardware.

### Reset potential and spiking threshold

Both, the biological threshold voltage  $V_{thresh}$  and the reset potential  $V_{reset}$  are translated to the hardware parameters  $V_t$  and  $V_{reset}$ , respectively. Both are calibrated values and are available for influencing neuron dynamics.

### Adaption and exponential term

Both, adaption and exponential activation are supported by the HICANN chip. Characterization and calibration of the adaption properties was done recently by *Friedrich* (2015). At the time of writing this thesis, the calibration was not integrated into the calibration framework and was therefore not accessible. Exponential activation was not

## 2 Towards uniform spiking rates

needed for the work of this thesis and is turned off in all measurements by using a LIF neuron model in PyNN.

### Synaptic weights

Synaptic weights are translated linearly from biological parameter to a 4 bit value on hardware. Therefore, only 16 discrete weight values from 0 to 15 are available on hardware. A biological value of  $weight \geq 0.2907$  nA corresponds to a hardware value of 15 and a biological value of  $weight \leq 0.0029$  nA to a hardware value of 0 for the *calibtic* version used. Note that both, the biological to hardware transformation and the effect of hardware value on circuit behaviour are changing as part of ongoing work.

### Synaptic delays

Delays on the hardware are not configurable but appear as a result of information processing times. Changing the delays in PyNN has no effect.

### Synaptic plasticity

Short term and long term plasticity mechanisms are part of the HICANN chip architecture. Short Term Plasticity (STP) calibration was recently developed by *Billaudelle* (2014). The calibration framework is not yet available and STP is not used in the work for this thesis.

## 2.2 Blacklisting

When emulating neurons on hardware, floating gate parameter variations and systematic hardware neuron to hardware neuron variations due to transistor mismatches result in significantly different spiking behaviour as shown in the introduction part of this chapter. The calibration aims to reduce these variations but since software is still in development, variations can still be high. In figure 2.2 we can see that some neurons do not spike at all while others seem to spike at roughly double the mean rate of all spiking neurons, although receiving the same external stimulus. Besides parameter variations and transistor mismatches defect hardware parts such as synapse drivers, bus lines or neuron circuits can cause this extremely different behaviour of some hardware neurons. It is therefore important to be able to identify hardware parts that do not work as necessary for a given application.

In this section some simple blacklisting methods are introduced to identify neurons which behave not as required.



### 2.2.1 Requirements

#### Number of neurons emulated on one HICANN chip at once

The amount of spike events that can be recorded from a single HICANN is limited. To extract spikes from a HICANN chip and send it to a host the so-called Layer 2 network is used. The connection between HICANNs and associated field programmable gate array (FPGA) can operate at 2 Gbit/s (*Schemmel et al., 2010*). At the time of writing this thesis the connection is operated at only 1 Gbit/s. In *Müller (2014)* the maximum spike throughput between HICANN and FPGA is calculated to be 55.6 MEvent/s for optimally packed spike events and a HICANN to FPGA operating bit rate of 2 Gbit/s.

In optimally packed spike events each packet contains two spikes. To be able to pack spike packets optimally small ISIs are needed. If the ISIs vary too much there will not be always 2 spikes in each packet. A double-spike packet requires 48 bit while a single-spike packet requires 27 bit. Additionally each packet requires 16 bit for header and cyclic redundancy check and 8 bit for pause after the packet (*Müller, 2014*). This results in an effective event size of  $(46 + 16 + 8)/2 = 36$  bit for double packed packets and  $27 + 16 + 8 = 51$  bit for only single packed packets.

Since in the measurements conducted for this thesis poisson sources were used, the ISIs of spiking neurons vary significantly and we can not assume optimally packed spike packets. In the worst case there will be only one spike per packet. The maximum spike throughput for optimally and worst packed packets can be calculated:

$$R_{\frac{1\text{spike}}{\text{packet}}} = \frac{\text{bandwidth}}{\text{event size}} = \frac{1 \text{ Gbit/s}}{51 \text{ bit}} \approx 19.6 \text{ MEvent/s} \quad (2.1)$$

$$R_{\frac{2\text{spikes}}{\text{packet}}} = \frac{\text{bandwidth}}{\text{event size}} = \frac{1 \text{ Gbit/s}}{36 \text{ bit}} \approx 27.8 \text{ MEvent/s} \quad (2.2)$$

These are the limitations for single HICANN usage. The neuromorphic platform is designed for wafer scale integration, allowing the routing of events through other HICANN-FPGA connections on the wafer. This will change the above calculated bandwidth limitations when all features of the neuromorphic platform are implemented.

Assuming single HICANN usage and filling 7 of 8 neuron blocks with spiking neurons of size 4, we would have  $4 \times 7 = 112$  neurons on one HICANN. With a speedup factor of  $10^4$  each neuron is limited to a firing rate of.

$$R_{\text{best}} = \frac{27.8 \text{ MEvent/s}}{10^4 \times 112} \approx 26.8 \text{ Hz} \quad (2.3)$$

$$R_{\text{worst}} = \frac{19.6 \text{ MEvent/s}}{10^4 \times 112} \approx 13.4 \text{ Hz} \quad (2.4)$$

To qualitatively determine the spike reduction when emulating many neurons on one

## 2 Towards uniform spiking rates

HICANN chip at once, following measurement is set up:

- All available neurons on one HICANN chip are emulated at once and their spike rate is measured.
- Then all neurons on only a certain number of neuron blocks are emulated at once and the measurement is repeated for the other neuron blocks until all hardware neurons are measured.
- This is repeated for different numbers of filled neuron blocks and the mean rate from all neurons is calculated.

In figure 2.3a the results of this measurement are plotted. A tendency towards lower spike rates can be observed when more neurons are emulated at once. But since a significant number of neurons do not spike at all the mean value is pulled down. In figure 2.3b the same data is shown but all neurons which did not spike in a separate blacklisting run with an input rate of 200 Hz are ignored. The blacklisting is described later in this section.

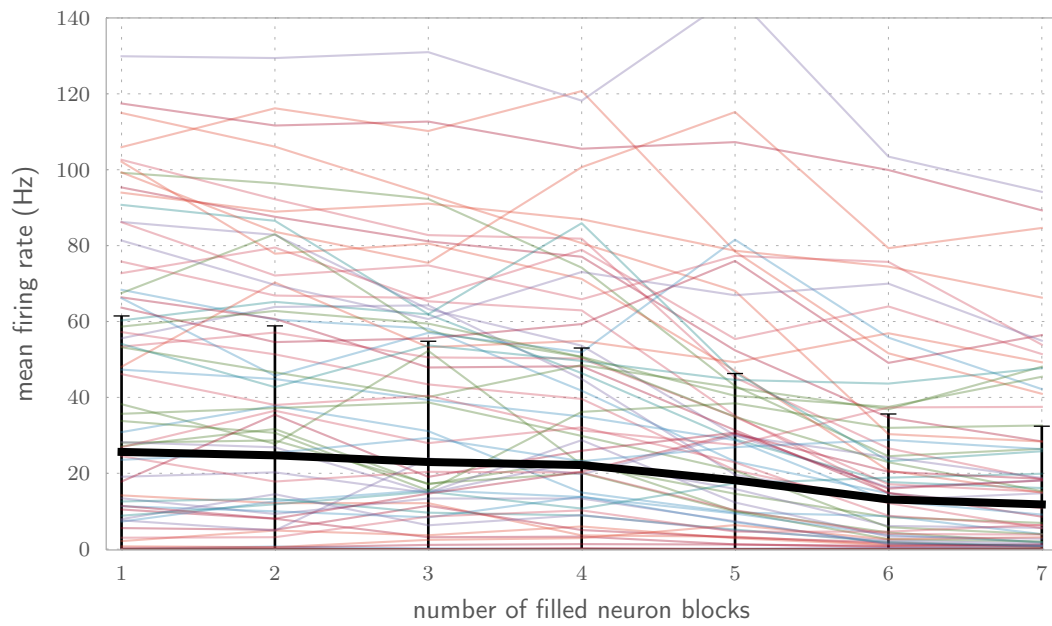
For 7 filled neuron blocks the mean rate of all neurons in figure 2.3a is  $\mu = 11.8$  Hz. With a speedup factor of  $10^4$  this results in a total event output of  $11.8 \text{ Hz} \times 10^4 \times 112 \approx 13.2$  MEvent/s. The same result can be obtained using the 61 neurons with a mean of 21.5 Hz shown in figure 2.3b. This value still lies below the maximum spike throughput calculated in equation 2.1. For the maximum throughput we assumed a constant rate though. In our poisson source, the rate varies resulting in varying firing rates in the neurons. Since all neurons receive the same poisson stimulus their firing rate should vary at best identical and at least correlated. Whenever the firing rate is high it can easily pass the maximum rate calculated in equation 2.4. This could be investigated in more detail by plotting the temporal evolution of firing rates, but is beyond the scope of this thesis.

### Blacklisting synapse drivers

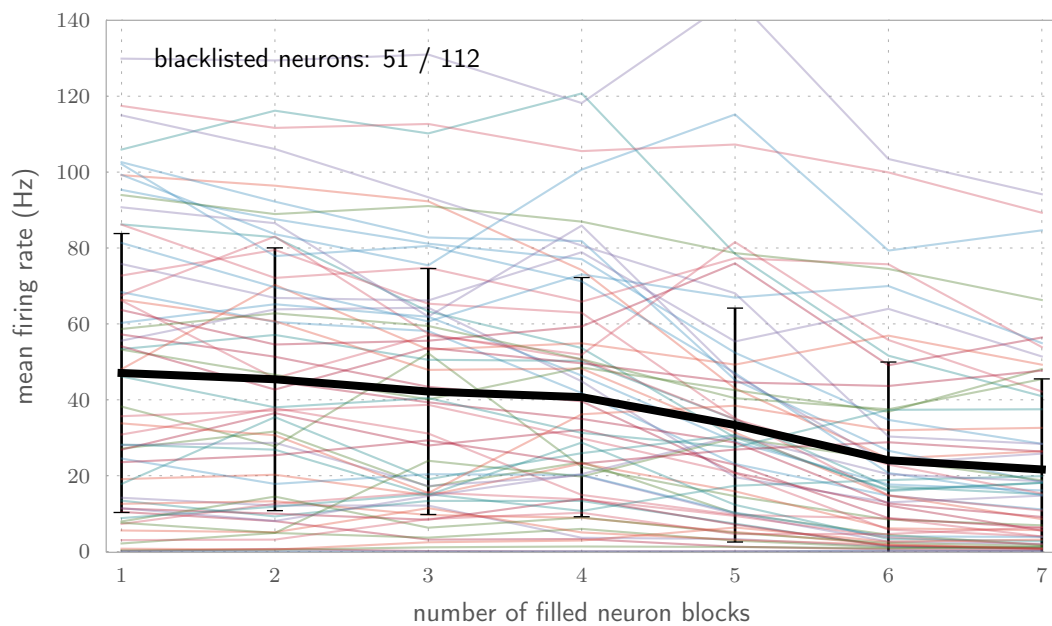
When conducting any kind of measurement with neurons having incoming synaptic connections, it is crucial that the synapse drivers forward incoming spikes event to the right target neuron. A *synapse driver defect detection tool* implemented by *Billaudelle (2014)* was used to detect synapse drivers, which do not encode addresses as required. In all measurements of this chapter there are no synaptic connections between neurons. And since all external spike inputs are routed through the digital network chip (DNC) link from output buffer 8, only one bus line is used in the layer 1 event network to route the input spikes to all neurons<sup>3</sup>. Before running any experiment the chosen synapse driver was tested with the defect detection tool and found to be working reliably.

---

<sup>3</sup>Whenever only one bus line is used, the routing algorithm in *marocco* chooses synapse driver 15.



(a) All neurons.



(b) Without not spiking neurons.

Figure 2.3: Mean firing rates for 112 neurons of size 4 on 7 neuron blocks of one HICANN. Each neuron receives the exact same input from a poisson source with a mean rate of  $\lambda = 200$  Hz. The x-axis indicates how many neuron blocks are filled with neurons per measurement step. In each measurement the same number of neuron blocks are filled and the measurement is repeated for different neuron blocks until all 7 neuron blocks are covered. For each data point the entire measurement is repeated 15 times. The colored lines connect the mean firing rates of the 15 repetitions for single neurons. The thick black line connects the neuron to neuron means for each measurement, the error bars indicate the neuron to neuron standard deviations. In figure (b) the same data is shown without not-spiking neurons. (From a separate blacklisting run as explained in section 2.2.2)

### 2.2.2 Method

In this section, two blacklisting methods are introduced and investigated for their applicability:

- blacklisting neurons which spike without external stimulus
- blacklisting not-spiking neurons for a given external stimulus rate

For any of these methods all 112 hardware neurons on one HICANN are emulated. Only 16 neurons on one neuron block are emulated parallel in one measurement step to avoid any spike loss. The neurons of each neuron block are emulated in a separate measurement.

#### Always spiking neurons

To find neurons which spike independent of external stimulus, neurons without any incoming synapses are emulated. Reasons for independently spiking neurons can be for example a bad calibration resulting in threshold voltages to be set below resting voltages. Then a measurement of 10 000 ms biological time is started and repeated for 5 times. Any neuron spiking at any of the emulation runs is marked as defect. The number of repetitions is arbitrary. 5 repetitions are chosen to make sure that neurons are marked which only sometimes spike as these neurons are expected to be more easily excitable. These neurons would have higher spiking rates for even low stimulus.

#### Not-spiking neurons

For most hardware emulations there are several not-spiking neurons. The number of not spiking neurons depends highly on the stimulus the neurons receive. Therefore, blacklisting runs with different stimulus rates were conducted.

Neurons spiking only sometimes are more likely to be blacklisted for less repetitions. Therefore, each measurement step was repeated only 2 times.

### 2.2.3 Results

First, all neurons on the HICANN are emulated without any connections. This measurement was repeated several times and there were never any spiking neurons without stimulus on HICANN 276. The same measurements were conducted also on the vertical setup<sup>4</sup>. Figure 2.4 shows the result of measuring all 112 available size 4 neurons on the HICANN on the vertical setup without any connections at all. 6 out of 112 neurons spiked without any stimulus input and are marked as defect.

In the next step, all neurons were emulated with external poisson input. For different external stimulus rates, all neurons on HICANN 276 which did not spike were marked as

---

<sup>4</sup>A setup where only a single HICANN chip is build in vertical setup and connected to a host. For this measurement the vertical setup connected to *porthos* was used.

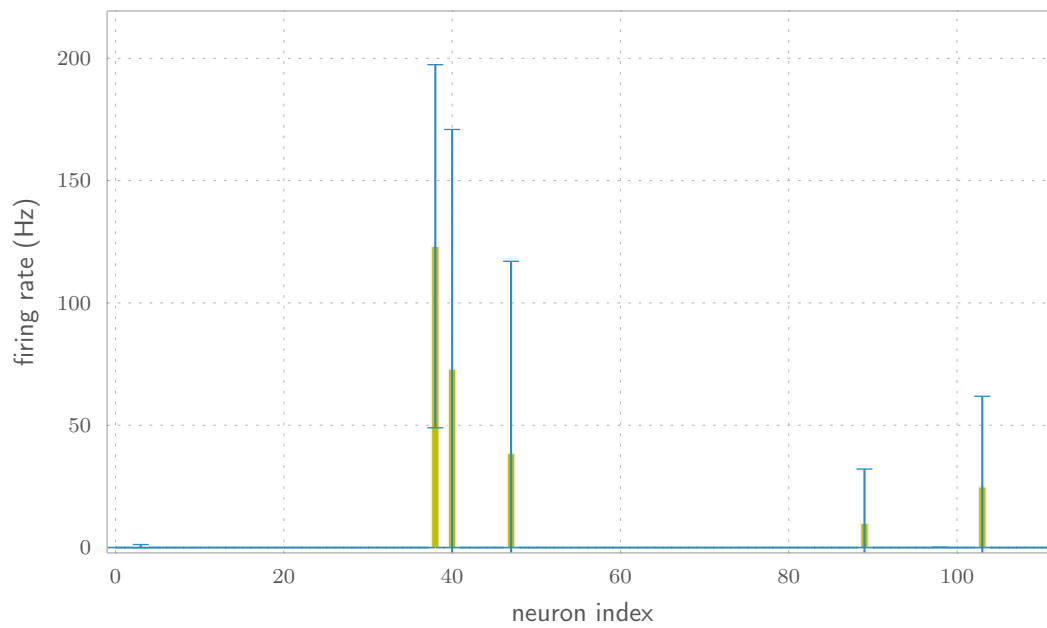


Figure 2.4: Measurement without any external stimulus. Mean and standard deviation of firing rates for still spiking neurons is shown. In each measurement step the 16 neurons of one neuron block are emulated at once. Each measurement step is repeated 5 times. These measurements were conducted on the vertical setup connected to *porthos*.

## 2 Towards uniform spiking rates

defect. In each measurement step only the 16 neurons on one neuron block were emulated at once.

In figure 2.5 exemplary results are shown for poisson rates  $\lambda = 40$  Hz and  $\lambda = 200$  Hz.

In figure 2.6 the number of not spiking neurons for different stimulus rates is shown. For stimulus rates below 20 Hz the number of not spiking neurons drastically decreases. Most neurons with the chosen neuron parameters (see appendix A) need more than one incoming spike to reach their threshold potential and emit a spike. When the rate is too low there is enough time for the membrane voltage to reach its resting potential between two incoming spikes. This would lead to not spiking of the neuron.

We can also see that the curve seems to move asymptotically towards a value just above 40% of not spiking neurons for high rates. All the neurons not spiking at low rates can be therefore characterized as neurons which just need more input but are not entirely idle.

In figure 2.7 all neurons from the measurement with a poisson rate of 200 Hz are plotted again and all neurons blacklisted in the 10 Hz and in the 40 Hz measurement are marked. We can see in figure 2.7a that the neurons marked in the 40 Hz measurement hardly spike at all for poisson input of 200 Hz. The roughly 10 neurons marked in the 40 Hz measurement but not marked at the 200 Hz measurement show rates close to zero. However, some of the neurons marked in the 10 Hz measurement do spike significantly for a poisson input of 200 Hz as can be seen in figure 2.7b.

Since for emulations of high spiking neurons on a single HICANN bandwidth limitations can be reached fairly easy (see section 2.2.1), it seems reasonable to conduct measurements on a lower rates. Therefore, for the following measurements mainly the blacklist from the 40 Hz measurement is used since it does not mark many neurons which would spike properly at higher rates.

The behaviour of neurons being blacklisted at lower rates but not at higher rates is also part of the investigated properties in section 2.3.

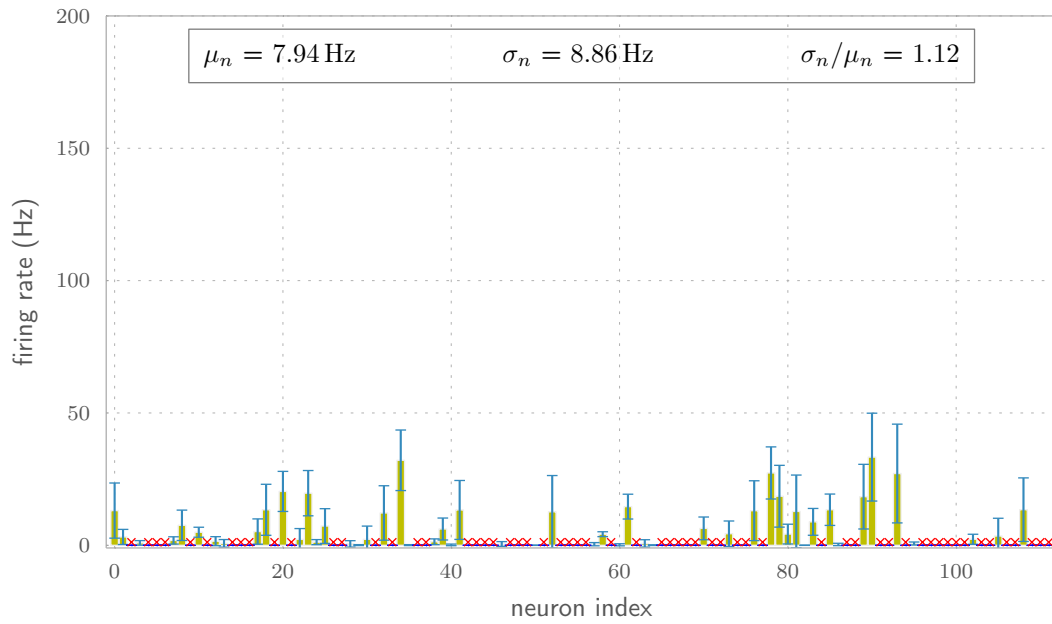
### 2.3 Investigating rate response to parameter changes

In the following section different parameters are varied to determine the resulting change in firing rates. The blacklisting results from section 2.2 are investigated by applying them to the measurement results of this section. To avoid spike loss in the parameter measurements in this section but not increase measurement times too much, the neurons of one HICANN are always measured in steps of 2 filled neuron blocks.

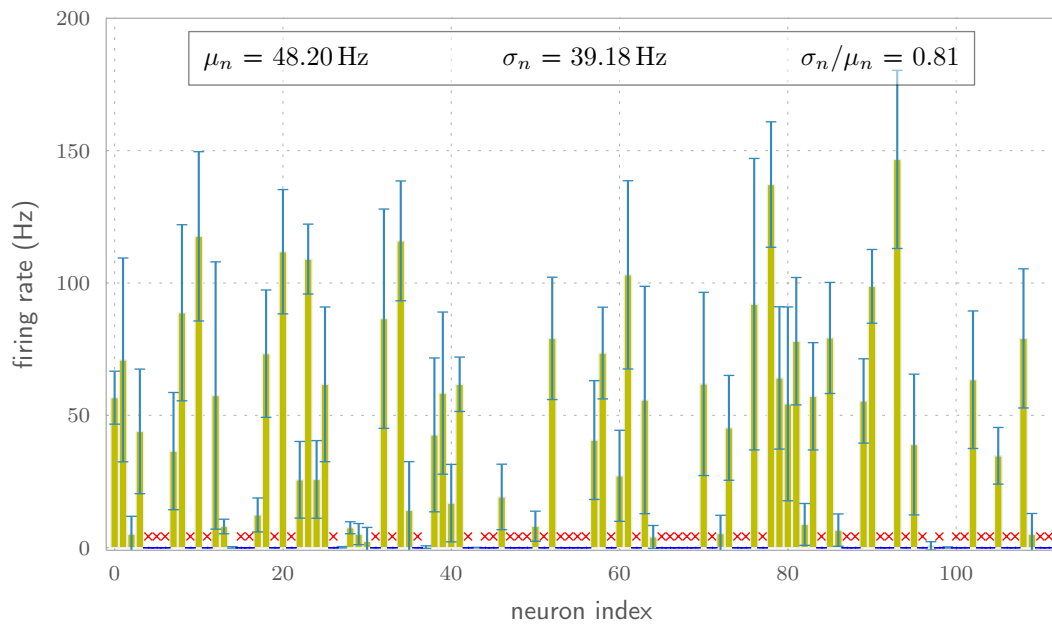
#### 2.3.1 Inputrate

To make a more general statement about firing rate dependencies of hardware neurons for the parameters given in appendix A, the same measurement as in section 2.2 was repeated with more repetitions. Each measurement was repeated 15 times to account for trial-to-trial variations. In figure 2.8a the result for all neurons is shown. In figures 2.8b, 2.8c and 2.8d the same data is plotted but only for neurons not blacklisted in blacklisting runs at 200 Hz, 40 Hz and 10 Hz, respectively (see section 2.2). We can see

### 2.3 Investigating rate response to parameter changes



(a) Poisson stimulus rate  $\lambda = 40$  Hz.



(b) Poisson stimulus rate  $\lambda = 200$  Hz.

Figure 2.5: Mean rates and standard deviations for 112 neurons of size 4 emulated on one HICANN. The red crosses mark not spiking neurons.  $\mu_n$  indicates the neuron to neuron mean firing rate and  $\sigma_n$  the standard deviation. Not spiking neurons are not used for mean and standard deviation calculations. Each neuron receives the same stimulus from a poisson source. In one measurement step only one neuron block of 16 neurons is emulated. Each measurement step is repeated 15 times.

## 2 Towards uniform spiking rates

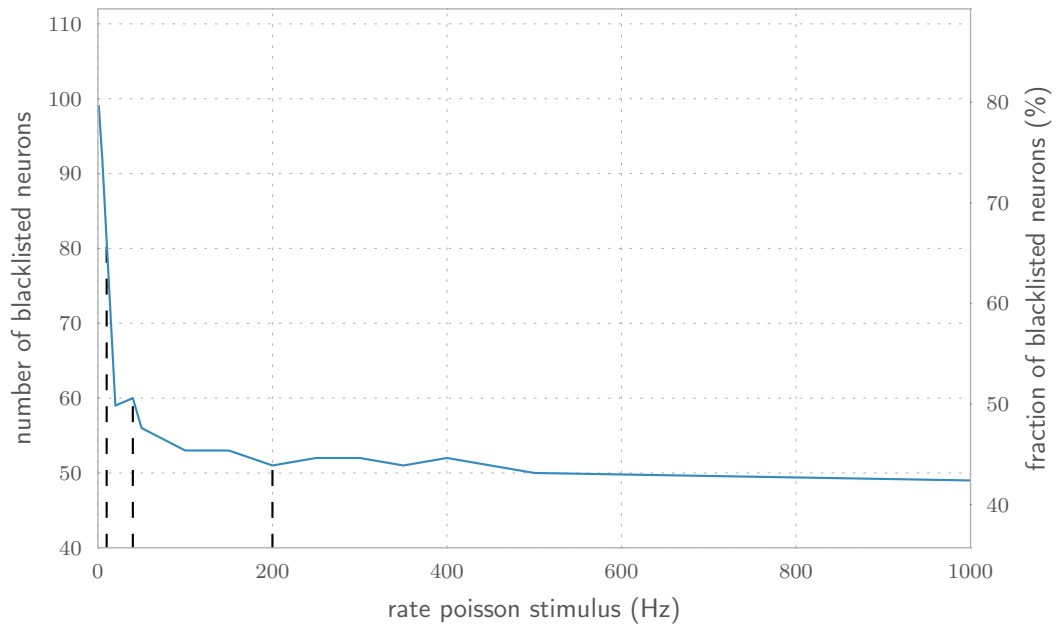
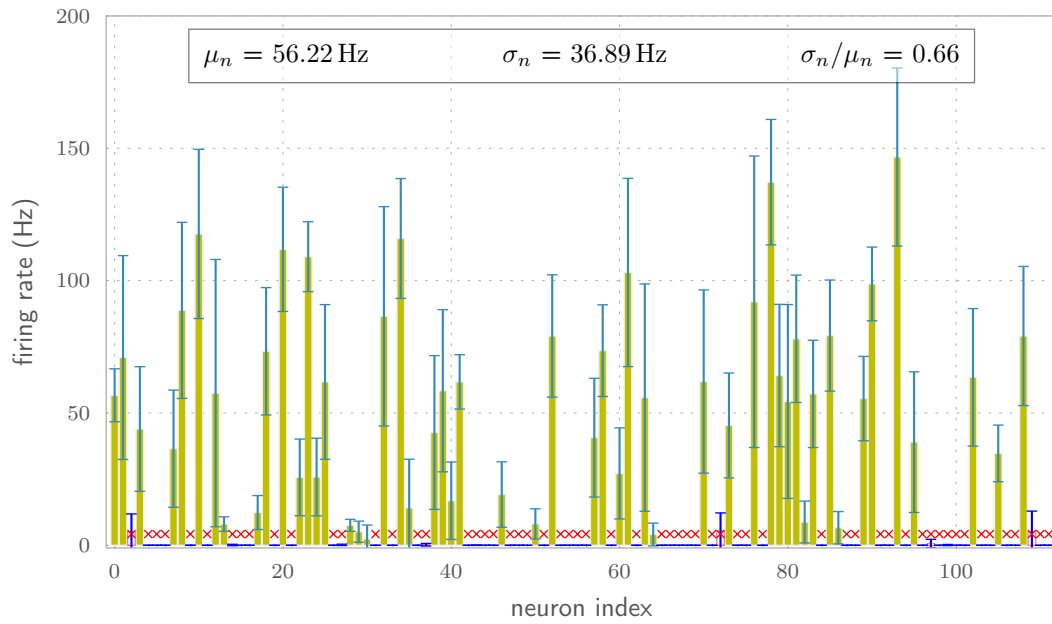


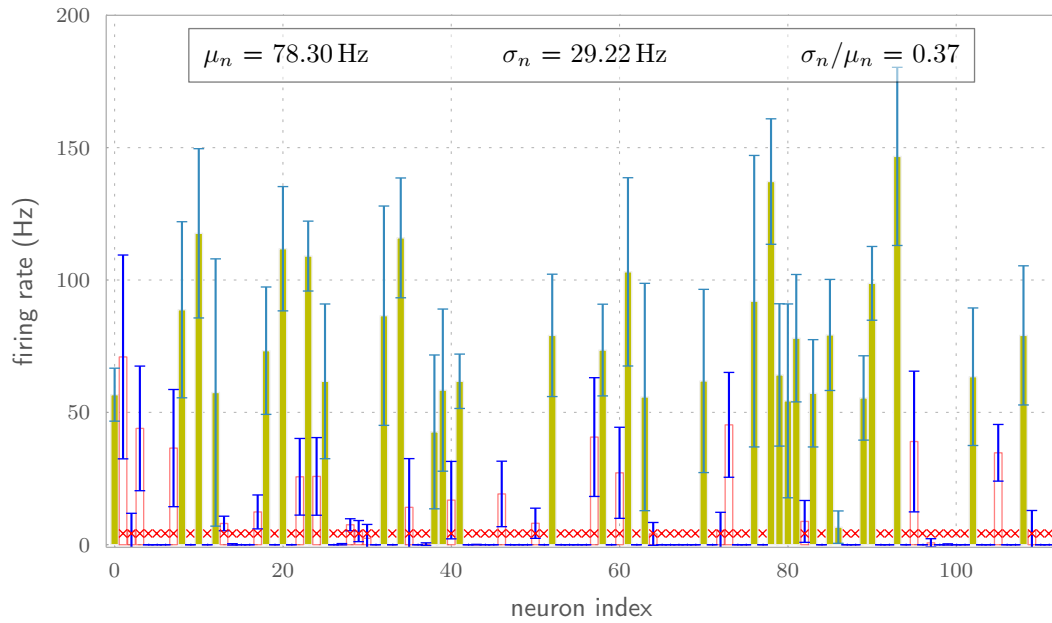
Figure 2.6: Number of blacklisted neurons for blacklisting measurements with different poisson source rates. Dashed lines indicate rates 10 Hz, 40 Hz and 200 Hz.



### 2.3 Investigating rate response to parameter changes



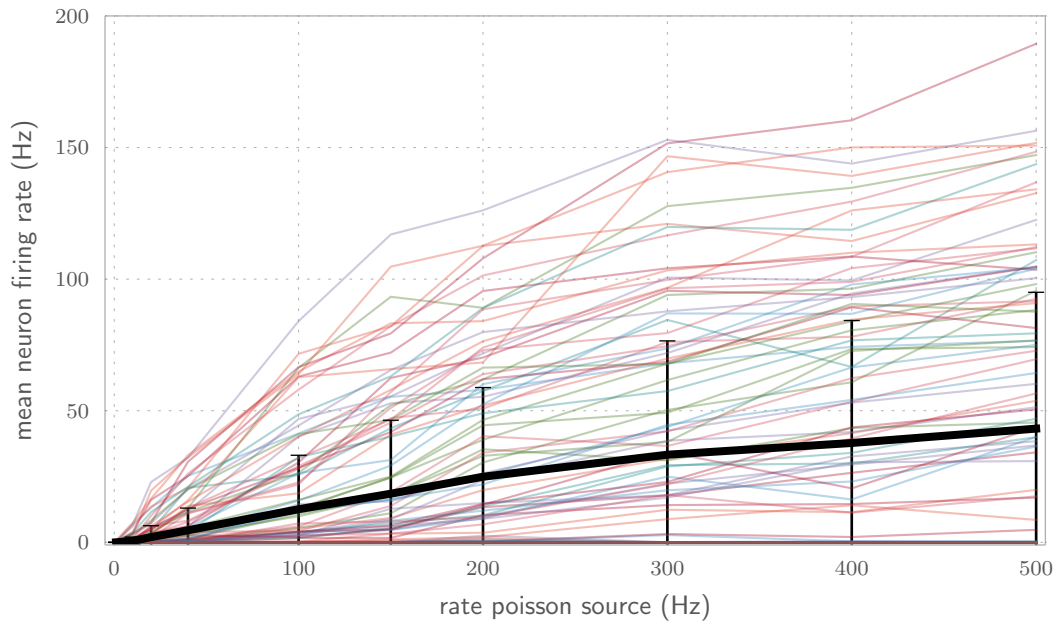
(a) Neurons from blacklisting measurement with 40 Hz are marked.



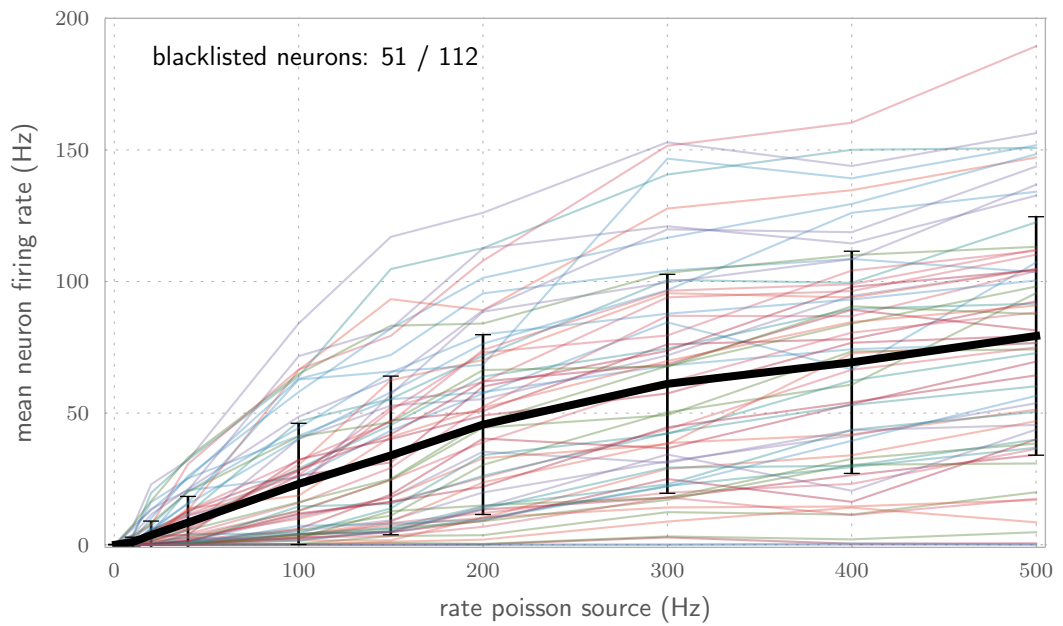
(b) Neurons from blacklisting measurement with 10 Hz are marked.

Figure 2.7: Rates plotted for poisson stimulus of  $\lambda = 200 \text{ Hz}$  for all 112 size 4 neurons on 7 neuron blocks of HICANN 276. The data is the same as used in figure 2.5b but a blacklist from the measurements with (a) 40 Hz and (b) 200 Hz are applied. The red crosses indicate neurons which did not spike in the corresponding blacklisting measurement.

## 2 Towards uniform spiking rates



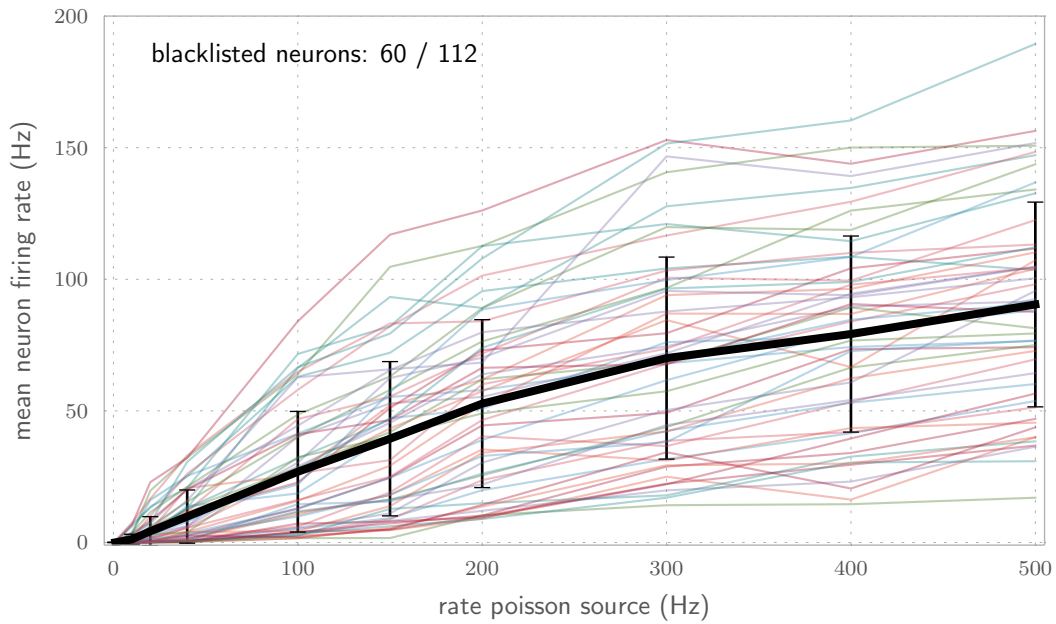
(a) Without any blacklisted neurons.



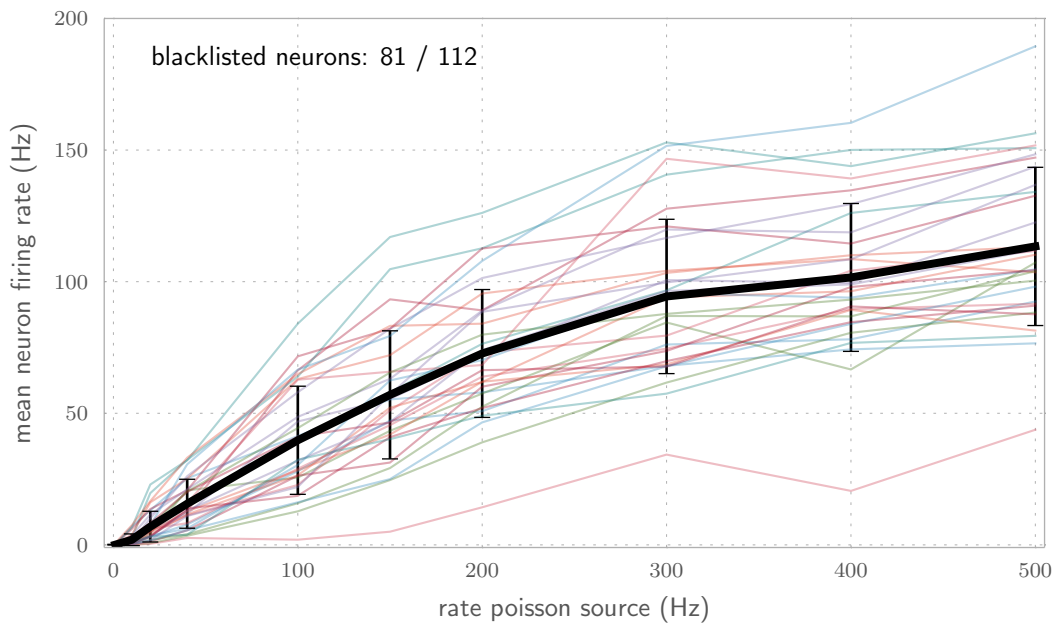
(b) Neurons not spiking at a stimulus rate of 200 Hz are blacklisted.

Figure 2.8: Firing rates dependency on stimulus rates, measured for 112 size 4 neurons on the first 7 neuron blocks of HICANN 276. In each measurements step 32 neurons on two successive neuron blocks are emulated. Each measurement step is repeated 15 times. The thick lines indicates the mean of all neurons and all repetitions, the error bars indicate the standard deviations. (continue next page)...

### 2.3 Investigating rate response to parameter changes



(c) Neurons not spiking at a stimulus rate of 40 Hz are blacklisted.



(d) Neurons not spiking at a stimulus rate of 10 Hz are blacklisted.

Figure 2.7: ... (start previous page) The faded lines in the background connect the means of 15 repetitions for each emulated neuron. The error bars indicate standard deviations across all neurons. In figure (a) all neurons are plotted. In figures (b), (c) and (d) the same data is plotted without neurons being blacklisted in previous blacklisting measurements (see section 2.2).

## 2 Towards uniform spiking rates

that the neurons blacklisted at lower rate blacklisting measurements are those neurons which show an overall lower mean spiking rate. When successively taken those neurons out, the mean spiking rate of all neurons for all trials increases.

### 2.3.2 Refractory time $\tau_{\text{refrac}}$

The refractory time  $\tau_{\text{refrac}}$  is the time for which a neuron can not be excited after it has emitted a spike. The biological value of  $\tau_{\text{refrac}}$  scales inversely with the pulse current  $I_{\text{pl}}$ . Thus, a higher value of  $I_{\text{pl}}$  results in a lower refractory time. The effect of  $I_{\text{pl}}$  on the refractory time  $\tau_{\text{refrac}}$  was investigated in *Schmidt* (2014). For values of  $I_{\text{pl}} > 200$  nA the refractory time only changed insignificantly. Therefore, in this measurement  $I_{\text{pl}}$  was varied in the range of  $0 \text{ DAC} < I_{\text{pl}} \leq 100 \text{ DAC}$ <sup>5</sup>. Figure 2.8a shows the results of measuring the  $I_{\text{pl}}$  dependency of the firing rates with a poisson stimulus rate of  $\lambda = 200$  Hz. For the same data, different blacklistings are applied. Like in previous measurements the overall rate increases for blacklistings measured at lower rates. And we can observe that the increasing of mean rate decreases with higher  $I_{\text{pl}}$ . This is in accordance with the results obtained in *Schmidt* (2014).

### 2.3.3 Synaptic weights

The synaptic weight is varied in the biological range in which all hardware values are covered as described in section 2.1.1. In figure 2.9 the results are plotted for two poisson stimulus rates  $\lambda = 200$  Hz and  $\lambda = 40$  Hz and different blacklisting data are applied. We can see that lowering the weight results in lower spiking rates. Thus, we can conclude that the intensity of incoming spikes is decreased for lower weights as intended by the hardware design.

### 2.3.4 Threshold voltage $V_{\text{thresh}}$

The threshold voltage  $V_{\text{thresh}}$  was investigated in previous work (*Alevi*, 2014) for very similar parameters. It was found that for voltage differences between resting and threshold voltages  $V_{\text{thresh}} - V_{\text{rest}} < 3$  mV the floating gate variations result in continuous spiking neurons. Higher distances decrease the spiking rate drastically. Since lowering spiking rates is not an issue of the investigations in chapter 3, decreasing  $V_{\text{thresh}}$  was not further investigated.

## 2.4 Summary

In this chapter it is characterized how a user of the HICANN wafer module can control neuron behaviour via access from PyNN. The characterization is based on the calibration and software available at the time of writing this thesis.

---

<sup>5</sup>Note that in *Schmidt* (2014) the current was given in nA while the parameter set in this work is given in DAC values. Conversion:  $1 \text{ nA} = \frac{2500 \text{ nA}}{1023} \text{ DAC}$ .

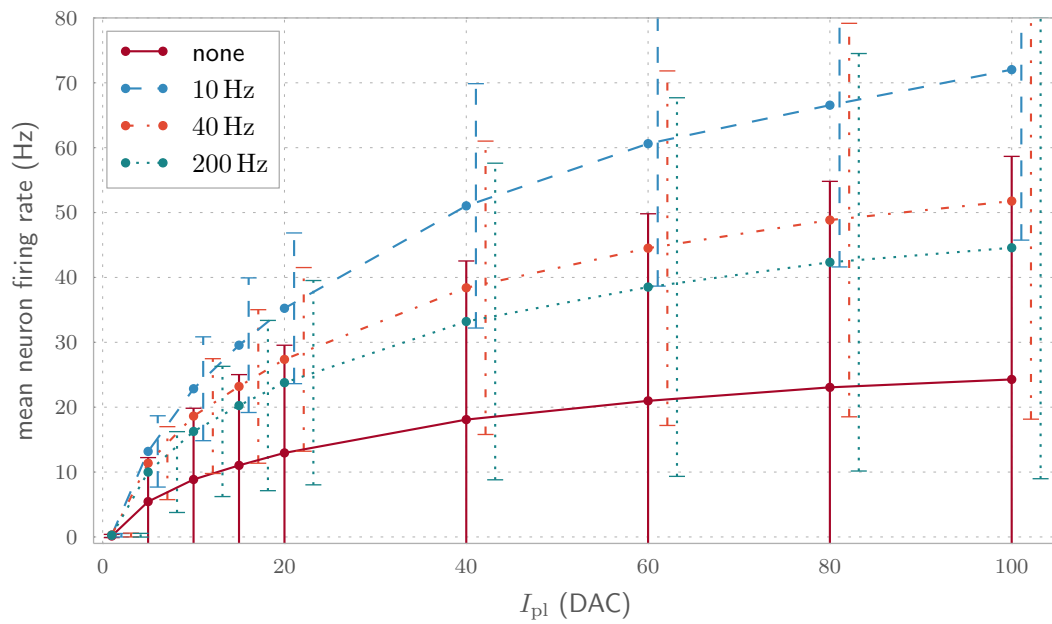
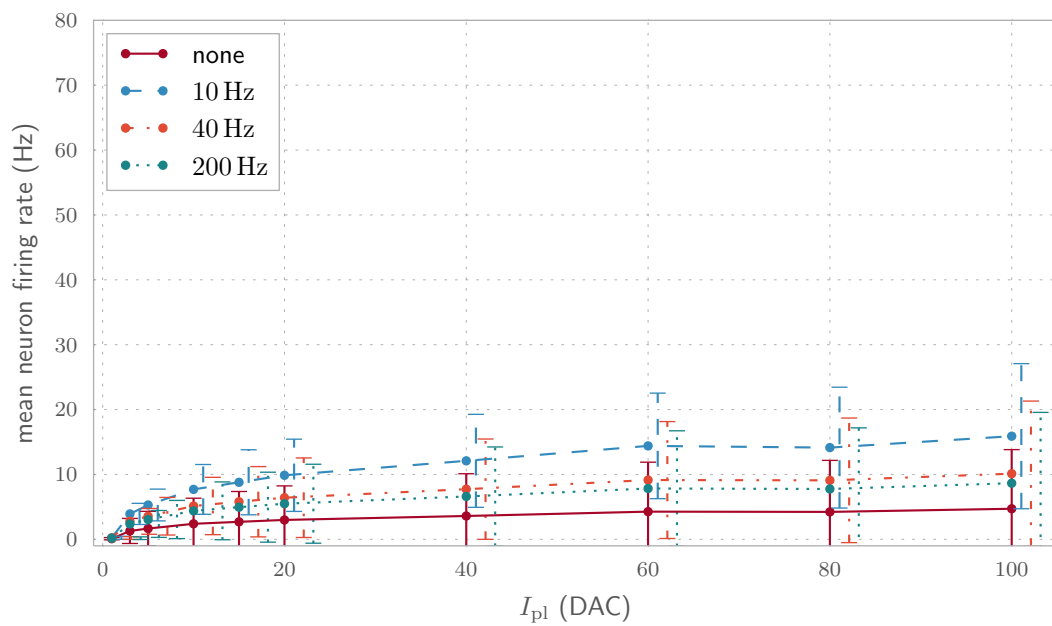
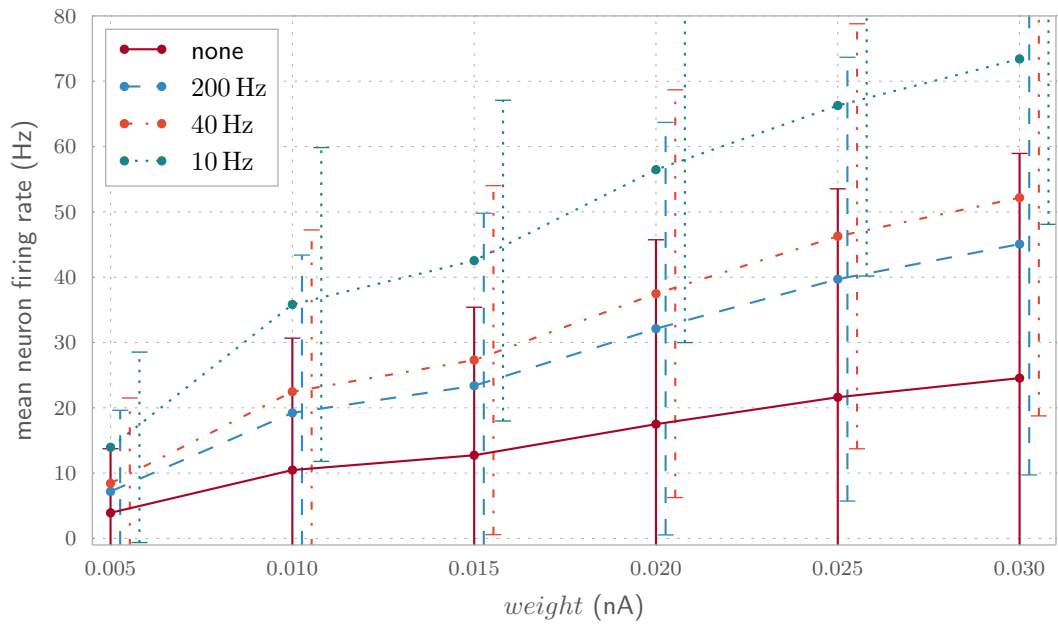
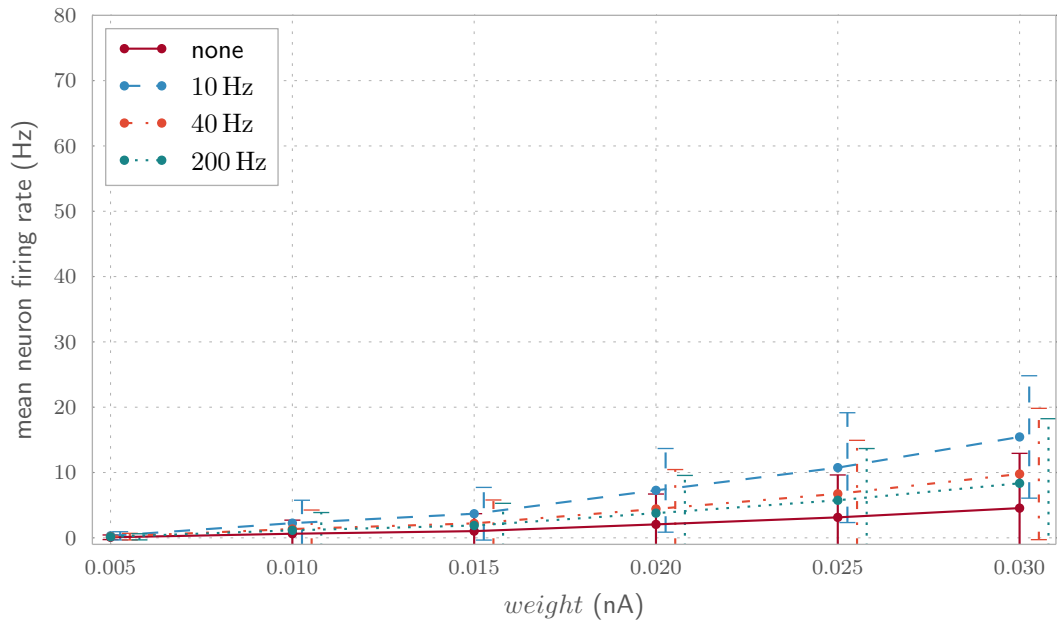
(a) Poisson stimulus rate  $\lambda = 200$  Hz.(b) Poisson stimulus rate  $\lambda = 40$  Hz.

Figure 2.8: Firing rate dependencies on the hardware current  $I_{pl}$ . The legend indicates which blacklisting data are applied to the experimental result. All 112 size 4 neurons on 7 neuron blocks on the HICANN 276 were emulated. In each measurement step 32 neurons on 2 neuron blocks were emulated at once. Each measurement step was repeated 15 times.

## 2 Towards uniform spiking rates



(a) Poisson stimulus rate  $\lambda = 200$  Hz.



(b) Poisson stimulus rate  $\lambda = 40$  Hz.

Figure 2.9: Firing rate dependencies on synaptic weight of the poisson source connection for stimulus rates  $\lambda = 200$  Hz and  $\lambda = 40$  Hz. The legend indicates which blacklisting data are applied to the experimental result. All 112 size 4 neurons on 7 neuron blocks on the HICANN 276 are emulated. In each measurement step 32 neurons on 2 neuron blocks are emulated at once. Each measurement step is repeated 15 times.

Some neuron parameters are currently calibrated towards maximizing the PSPs triggered by incoming spike events. Others are fixed at certain values to avoid uncharacterized influence on other parameters. (Section 2.1.1) These preliminary calibration methods result in many properly spiking neurons and disable uncontrollable behaviour but at the cost of influence by the user using the PyNN interface. Then some parameters are still being characterized or developed calibration methods need to be implemented in the software stack.

These prerequisites leave only a few parameters to control neuron behaviour. These are:

- $I_{pl}$  controlling the refractory time  $\tau_{refrac}$
- Threshold voltage  $V_{thresh}$
- Reset potential  $V_{reset}$
- Synaptic weight

Synaptic plasticity mechanisms as well as adaption and exponential activation are also available but have not been investigated in the scope of this thesis. The parameters  $E_{rev,E}$ ,  $E_{rev,I}$  and  $V_{rest}$  are not fixed by the calibration but changing their values can undo the calibration benefits. This could be investigated in more detail but is not done in this thesis.

Despite the available calibration methods, some neurons do still vary significantly. Neuron to neuron standard deviation to mean ratios of above 1 can be measured. Some neurons do not spike at all for different parameter settings or spike independent of receiving stimulus. A blacklisting method was used to mark all neurons not spiking for different stimulus rates (Section 2.2). Neurons not spiking when receiving an external stimulus of 40 Hz were found to spike either not or at least only very rarely even for higher rates. Some of the neurons not spiking with an external stimulus of 10 Hz did spike reasonably for higher rates, though. The number of not spiking neurons did only decrease slightly for rates higher than 200 Hz while increasing rapidly for rates below 40 Hz (see figure 2.6). Therefore, a blacklist created from not spiking neurons at 40 Hz external stimulus is used throughout the measurements of this thesis. When seen suitable results using blacklists created at stimulus rates of 10 Hz or 200 Hz are used for comparison.

In section 2.3 the available parameters listed above are swept within their dynamic ranges. All the investigated parameters are able to influence the spiking rate of neurons. When more neurons are blacklisted and not taken into account for calculating the mean spiking rates, the influence of parameter change is higher. When less neurons are blacklisted, more not spiking neurons depress the mean spiking rate.





## 3 Emulating a recurrent neural network

In previous work (*Alevi, 2014*), a basic feed forward chain network was emulated on the HICANN wafer module. That chain network was build in a way, that the only requirements for it to work are firing neurons and a working spike transport through the layer 1 event network. By choosing parameters for which neurons in the network spike at high rates, the network behaves as intended and spikes are passed through different populations.

In this chapter the competitive dynamics in a recurrent network are investigated. The network is intended to behave similar to a soft Winner Take All (sWTA) network. The chosen network is inspired by the sWTA network investigated in *Pfeil et al. (2013)*. As a first step we chose a slightly more simple network then described in the paper.

Neuron-to-neuron standard deviation to mean ratios rarely drop below 0.4, even with blacklisting methods marking 70% of the hardware neurons as not behaving as required. Since the neuron number per population is limited with only one HICANN used and the neuron-to-neuron deviations are so high, connection probabilities below 1 are avoided in the chosen network.

The inter HICANN routing had only been used for the above mentioned chain network at the time of conducting these experiments. To avoid uncharacterized influences, the network was emulated on only one HICANN chip.

### 3.1 Network Topology

soft Winner Take All (sWTA) networks are characterized through competitions for activity in different subunits. In this network the competition is realized through two equal sized populations being inhibitory connected to each other. Each neuron inhibits each neuron of the other population. Each population is then excited by a different external poisson source. The network topology is drawn in figure 3.1. To decrease the effect of neuron-to-neuron variations, connection probabilities are chosen to be all  $p = 1$ .

This network topology is expected to result in the higher stimulated population to suppress the other population. Consequently the other population would inhibit the first one less. Depending on the strength of the inhibition and difference of external stimuli the both populations receive, this will result in a certain difference in mean firing rates between the two populations. For strong inhibition and high stimulus differences one population should entirely inhibit any spiking in the other population.

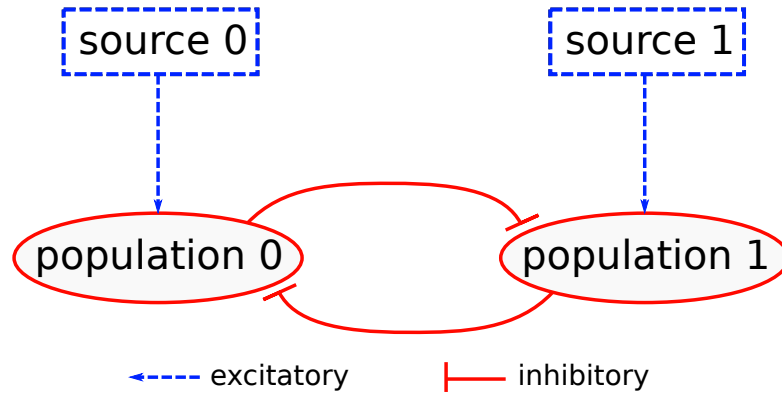


Figure 3.1: Network topology of the emulated sWTA network. All neurons available after blacklisting are split into two populations. All neurons of each population are connected inhibitory to all neurons of the other population. Each neuron in one population receives external stimulus from the same poisson source.

## 3.2 Methods

### 3.2.1 Choosing the neurons for each population

The methods in this section intend to find two populations behaving similar when receiving the same stimulus. To ensure that the two population behave similar, all neurons available after blacklisting are sorted by their spiking rate for a chosen stimulus. Then every second neuron is chosen to belong to population 0 and every other neuron to population 1 to get a similar overall mean spiking rate. For the following measurements, the measurement results from the blacklisting run with a poisson stimulus of  $\lambda = 40$  Hz are used (see section 2.2).

This method depends on the spike data which is used to determine the spike rates. It is therefore only a rough approximation of spiking behaviour which effect will be investigated in the result section.

Note that the neurons of the two populations are now randomly placed across the HICANN.

### 3.2.2 ESS vs. HICANN

Most measurements in this chapter are simulated with the ESS backend first and then compared with emulation results on the HICANN. The ESS simulations in this work assume ideal hardware neurons without neuron-to-neuron variations.

To simulate a network on the ESS no changes to the (PyNN) script are necessary. This made it possible to investigate the ideal behavior of the network beforehand and prototype the analysis.

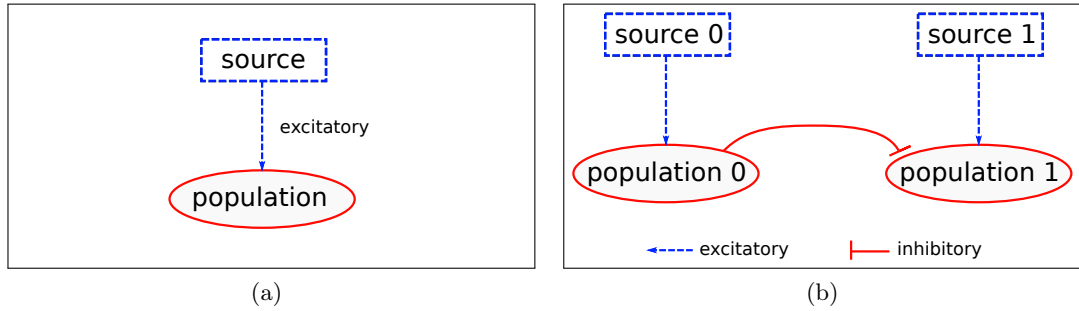


Figure 3.2: Independently measured parts of the sWTA network.

### 3.2.3 Investigating different parts of the network

At first only subunits of the network are investigated individually. In the first step only one population is emulated receiving external stimulus from a poisson source as shown in figure 3.2a. This is done for both populations separately to examine if the neuron sorting yielded the intended result.

In a second step, the network is emulated with only one population being inhibitory connected to the other while not receiving inhibitory input itself. The setup is shown in figure 3.2b.

At last, the entire network as shown in figure 3.1 is emulated and investigated.

### 3.2.4 Investigated network properties

For the following investigations the entire network is emulated.

#### Point of equal firing rates

The first characterization is motivated by the investigations in *Pfeil et al. (2013)*. One population receives external stimulation at constant rate while the other populations external stimulus is varied. Both populations firing rates are then plotted in dependence of the varied external stimulus. For identical populations the firing rates should be on average equal when both populations receive the same poisson input.

## 3.3 Results

After having done all measurements and while writing this thesis a bug in the simulation script was found. Unfortunately the blacklisting was not applied correctly and the neurons of the populations were chosen randomly. The following results therefore include non spiking neurons. In the end of the chapter some results from measurements with correctly applied blacklisting are shown and compared.

The hardware settings for measurements are the same as explained in the introduction part of chapter 2. Thus, there can be 112 neurons emulated on one HICANN.

### 3 Emulating a recurrent neural network

In this section the blacklisting data gained from the measurements at 40 Hz is used (see section 2.2). Therefore, 60 neurons are blacklisted and 52 are available for experiments. The same measurement data used for the blacklisting is also used to sort the available neurons by their rates into two similar spiking populations as explained in section 3.2.1. Each population consists therefore of 26 neurons.

#### 3.3.1 Only one population with poisson stimulus

To evaluate the success of the sorting, both populations mean firing rates are measured for different stimulus rates. The results are shown in figure 3.3. The standard error of the mean after 15 repetitions is assumed to be negligible compared to the neuron-to-neuron variations. Hence, only the error bars of the neuron-to-neuron standard deviations are plotted.

We can see that population 1 spikes roughly 5 Hz higher for stimuli above 10 Hz than population 0 does. The effect of the rate difference will be examined in the following.

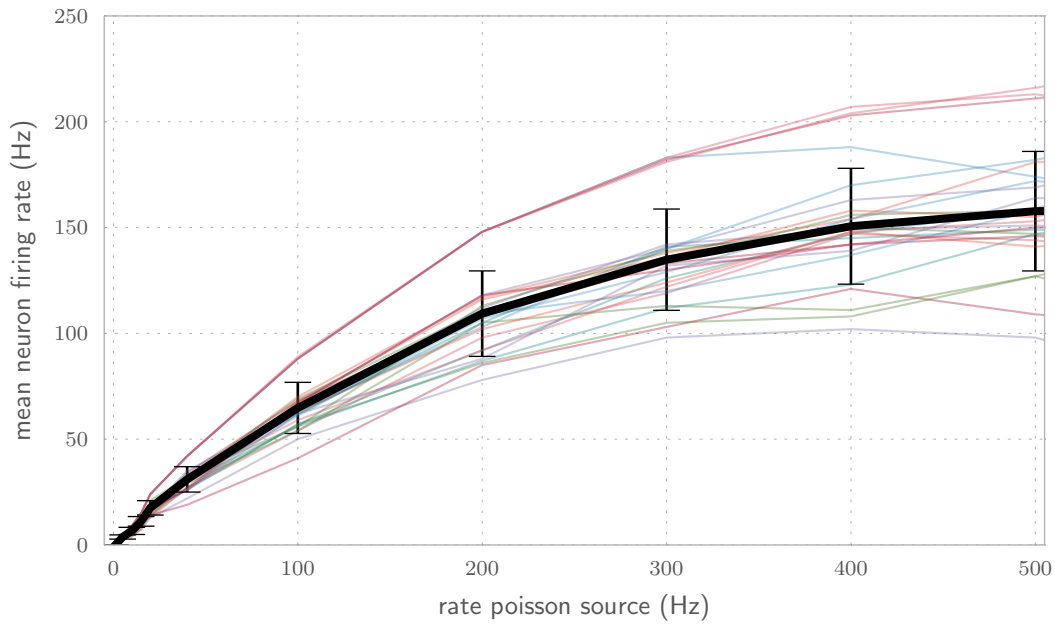
Figure 3.3a shows the same measurement with the ESS backend. The tendency of less increasing spiking rate for higher stimulus input is in agreement with the hardware results. But the ESS neurons spike at much higher rates. The reason is that ideal neurons are simulated.

Figure 3.10a shows an exemplary voltage trace of one neuron from the described setup, illustrating the correlation of stimulus events and membrane response.

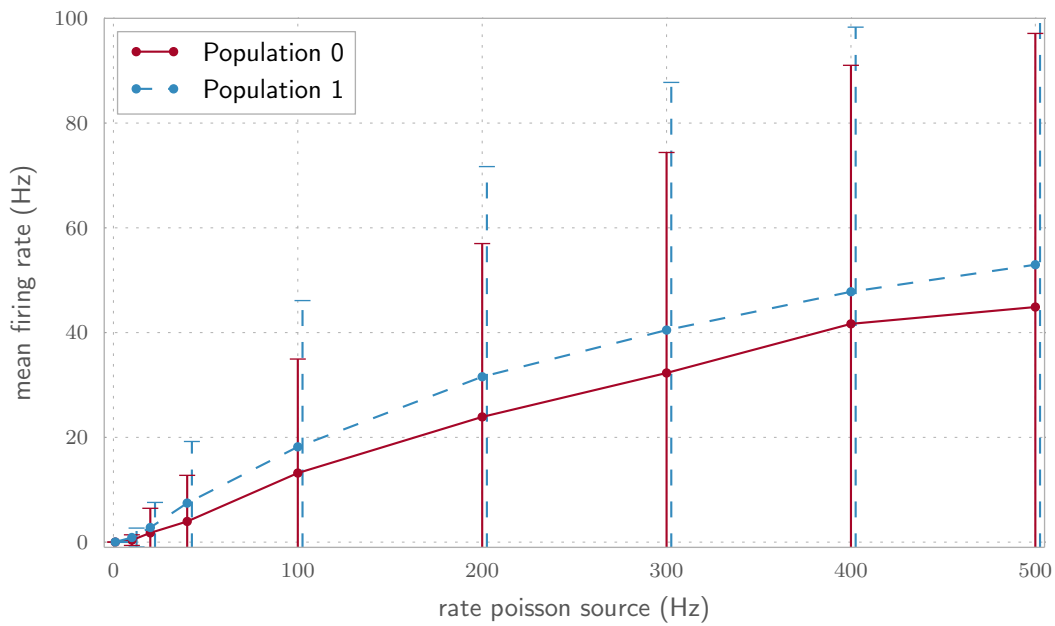
#### 3.3.2 Two populations with only unidirectional inhibitory connections

To determine the effect of different strength of inhibitory input without any recurrent connections, both populations are emulated but only one population inhibits the other one and not vice versa. For one stimulus at constant rate and the other at varied rates the populations mean rates are investigated. The measurements were again conducted on both, the ESS and the hardware. Results are shown in figure 3.4.

We can see that both, ESS simulation and hardware emulation show similar behaviour. Population 0 spikes at the same mean rate as population 1 when population 0 receives external stimulus at 21 Hz and population 0 receives external stimulus at 50 Hz but also inhibitory input from population 1. The point of same spiking rates in simulation and emulation is in good accordance. figure 3.4b is zoomed into the relevant range. In appendix B the plot can be seen. We can see that there are some neurons spiking at high rates and some at very low but in between is a gap. The reason could be the missing blacklisting which might have marked the low spiking neurons as defect. A main difference between hardware and simulation can be found again in overall spiking rate and in the neuron-to-neuron deviations. The neurons from the ESS measurement spike much stronger. Another very important observation is, that the effect of inhibition in the hardware emulation is much less than in the ESS simulation. While the inhibited populations mean rate goes down to low rates already for rates of  $\lambda_0 = 50$  Hz for the ESS simulation, in the hardware emulation the decrease is less steep and continues almost linear until a population 0 stimulus rate of 100 Hz.



(a) Simulation with the ESS



(b) Measurements on the HICANN

Figure 3.3: Only one population is emulated and receiving poisson stimulus at different rates. Figure (a) shows the simulations on the ESS. Only one population is shown since both mean firing rates are the same. The faded lines indicate single neurons. The thick, black line is the mean of all neurons and the error bars indicate the neuron-to-neuron standard deviations. In figure (b) the relevant range of the hardware results are shown. In appendix B the full plot can be found. Each line indicates the results of one population, both measured in separate runs. The plotted data points are the means of all 26 neurons firing rates which are determined as the means of 15 repeated measurements. The error bars indicate the standard deviations across the 26 neurons.

### 3 Emulating a recurrent neural network

In figure 3.5, the results of the same experimental setup are shown for a higher constant poisson rate of population 0. The point of equal firing rates are shifted by roughly 10 Hz between ESS simulation and hardware emulation. This could be caused by the different overall firing rates show in figure 3.3, due to the wrongly applied blacklisting. Additionally the point of equal firing rates is shifted to a higher stimulus compared to the measurement in figure 3.4 as would be expected. But one has to be careful with the conclusions from these plots since in close range of the crossing of both plots there are only few data points.

#### 3.3.3 Emulating the entire network

In the final step the entire network is emulated. The ESS simulation results shown in figures 3.6 and 3.7 are in surprisingly good agreement with the hardware measurements. But this could be coincidence since in the plotted range there are only two data points for the hardware measurement. The only significant difference is the overall firing rate of the populations which differs by a factor of 2 to 5 depending on the stimulus rates since the firing rates on the hardware saturate faster than the ESS simulation assumes.

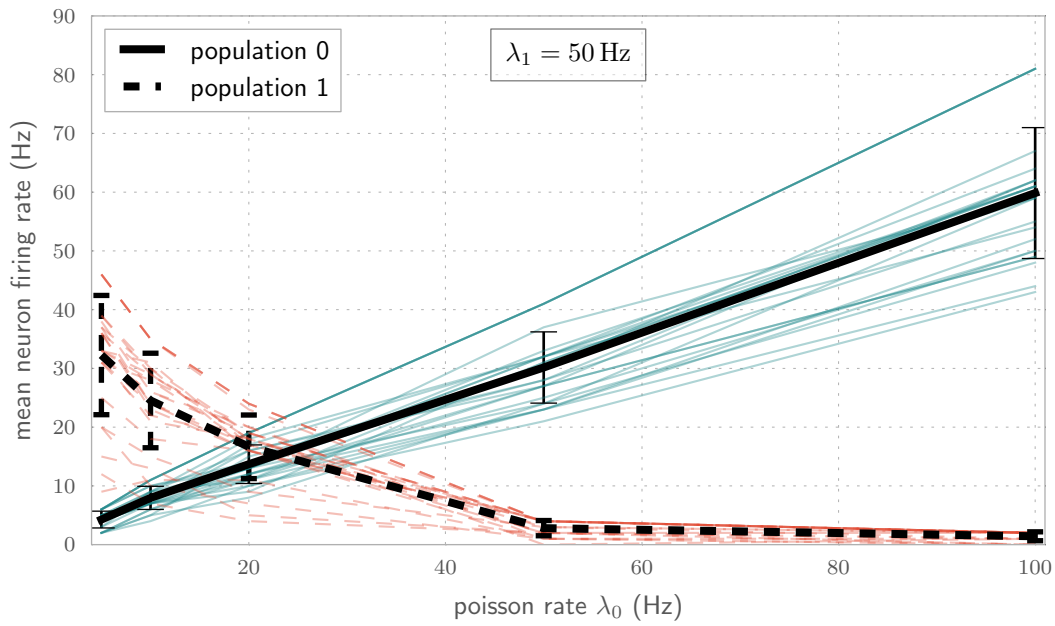
#### 3.3.4 Results with correctly applied blacklisting

After fixing the experiment software to correctly apply the blacklisting data, some measurements were repeated. In figure 3.8 both populations independent mean rates are shown for different stimuli. The difference between the mean rates is lower than it was with the wrong blacklisting applied.

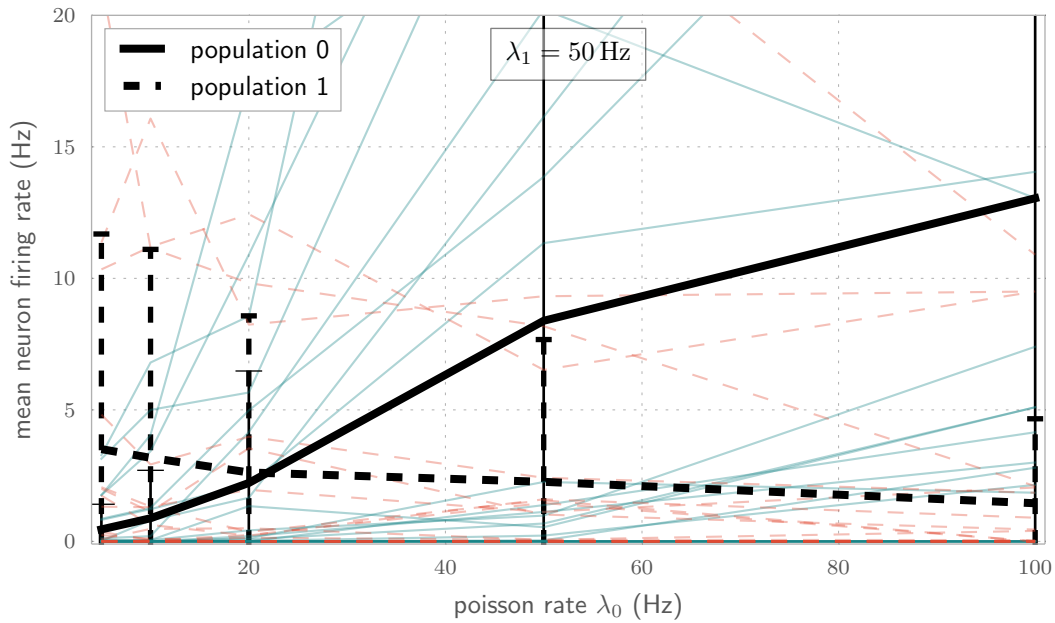
#### 3.3.5 Observation of network behaviour on neuron level

In figure 3.10b the voltage trace and incoming and outgoing spike events are shown for one exemplary neuron. The plots only show a short period of the simulation time. The correlation of incoming stimulus spikes and registered spikes of the neuron itself can be seen. And the inhibitory effect of inhibitory spike events from the other population can also be observed.

In figure 3.11 a raster plot is shown where all spike events in the network can be seen. For this plot a measurement with correct applied blacklisting was used. In this experiment run one population receives the usual poisson stimulus with constant rate  $\lambda = 50$  Hz. The other population receives a stimulus which rate increases with the time from  $\lambda = 1$  Hz to  $\lambda = 300$  Hz. It can be observed how the spike amount in the population with constant stimulus decreases when the other populations stimulus increases. Also the inhibition is delayed from the increasing stimulus since the stimulated population first needs to increase its own rate while overcoming the other populations inhibition. And then its own inhibition will effect the other population.



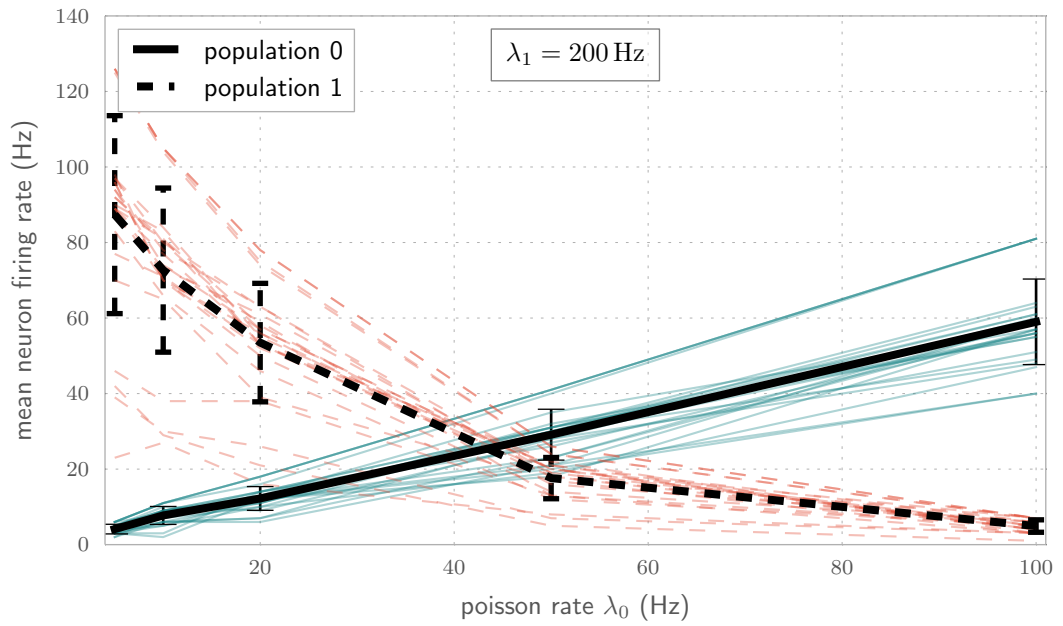
(a) Results from ESS measurement



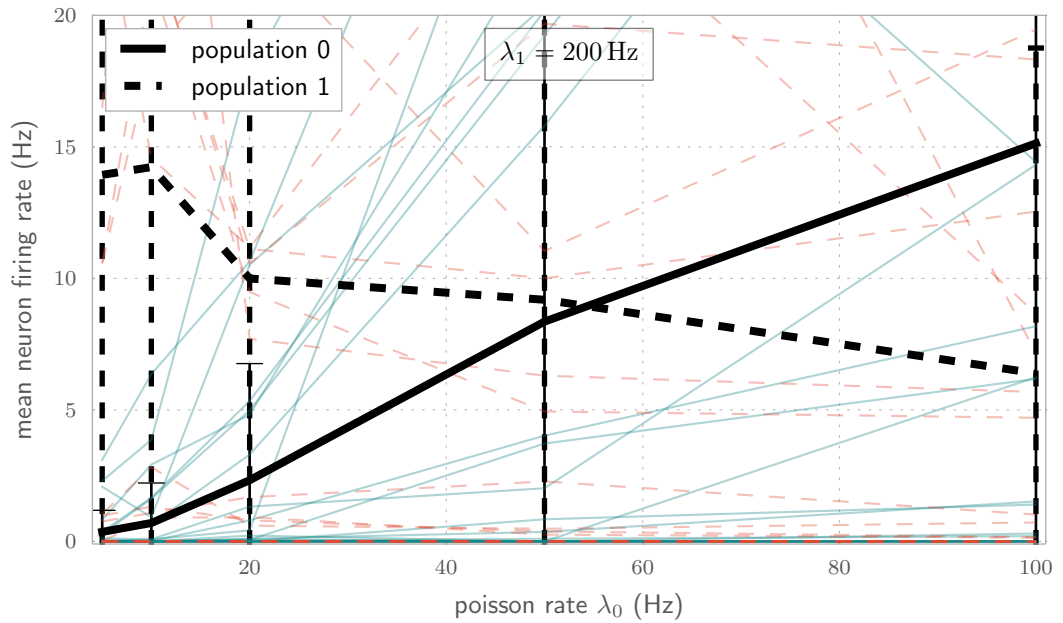
(b) Results from hardware measurement

Figure 3.4: Two populations are emulated but only population 1 receives inhibitory input from the population 0 as shown in figure 3.2b. The network is emulated for different population 0 stimuli  $\lambda_0$ . The poisson stimulus for population 1 is constant at  $\lambda_1 = 50$  Hz. The faded lines in the background are the means of 15 repeated measurements for each single neuron. The thick lines indicate the means of all neurons of one populations, error bars indicate the neuron-to-neuron standard deviations. The solid lines belong to population 0 and the dashed lines to population 1. Figure (b) is a zoom in the relevant ranges. The full plot can be found in appendix B.

### 3 Emulating a recurrent neural network



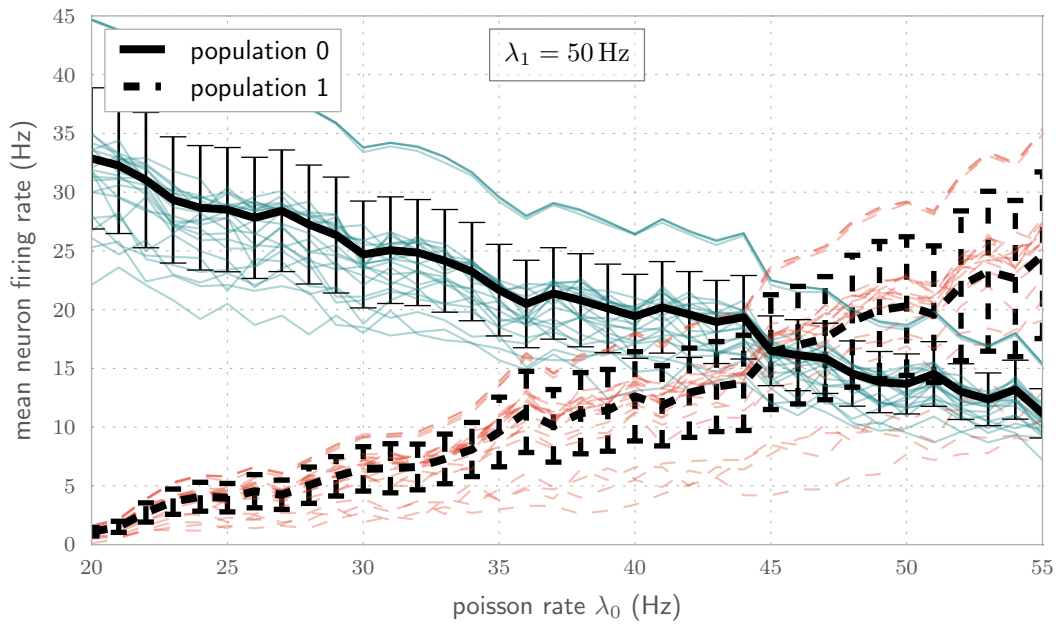
(a) Results from ESS measurement



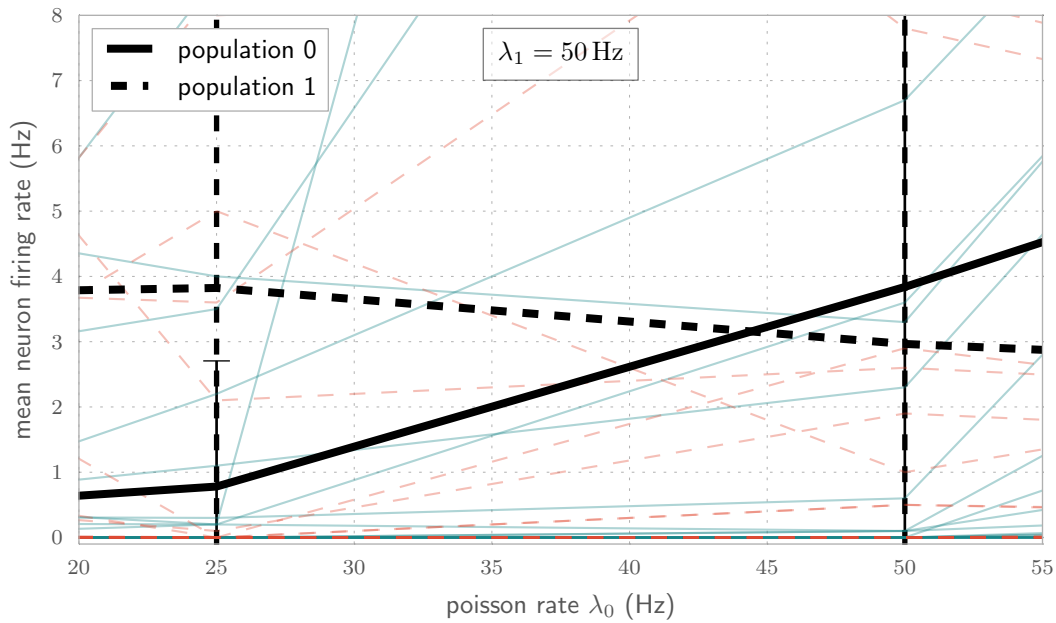
(b) Results from hardware measurement

Figure 3.5: Two populations are emulated but only population 1 receives inhibitory input from the population 0 as shown in figure 3.2b. The experimental setup is the same as described in figure 3.4 but with population 1 receiving a poisson stimulus of rate  $\lambda_1 = 200$  Hz. Figure (b) is a zoom in the relevant ranges. The full plot can be found in appendix B.





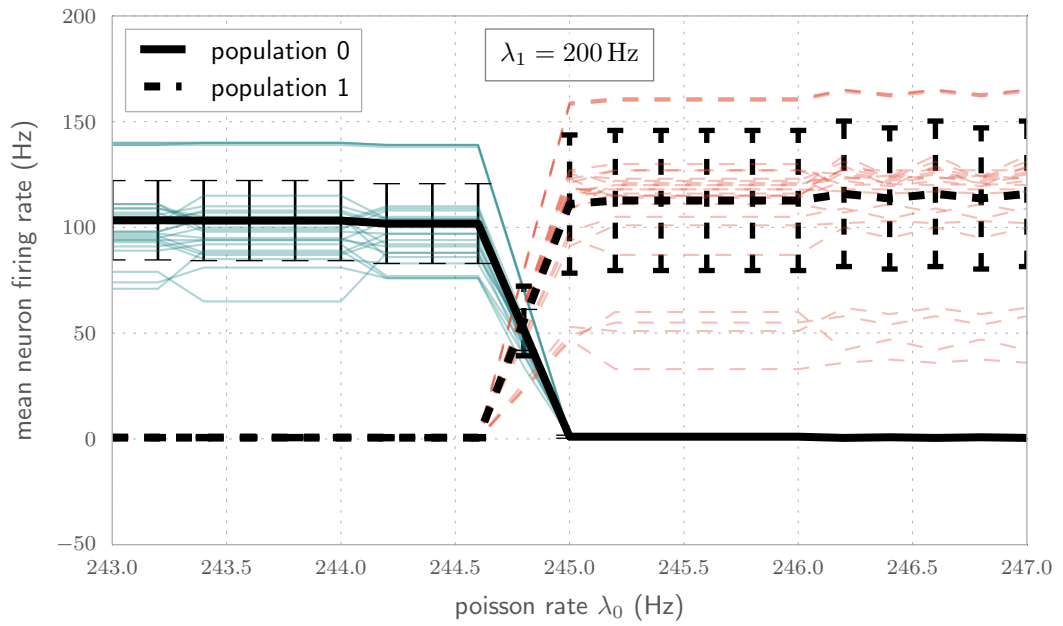
(a) Results from ESS measurement



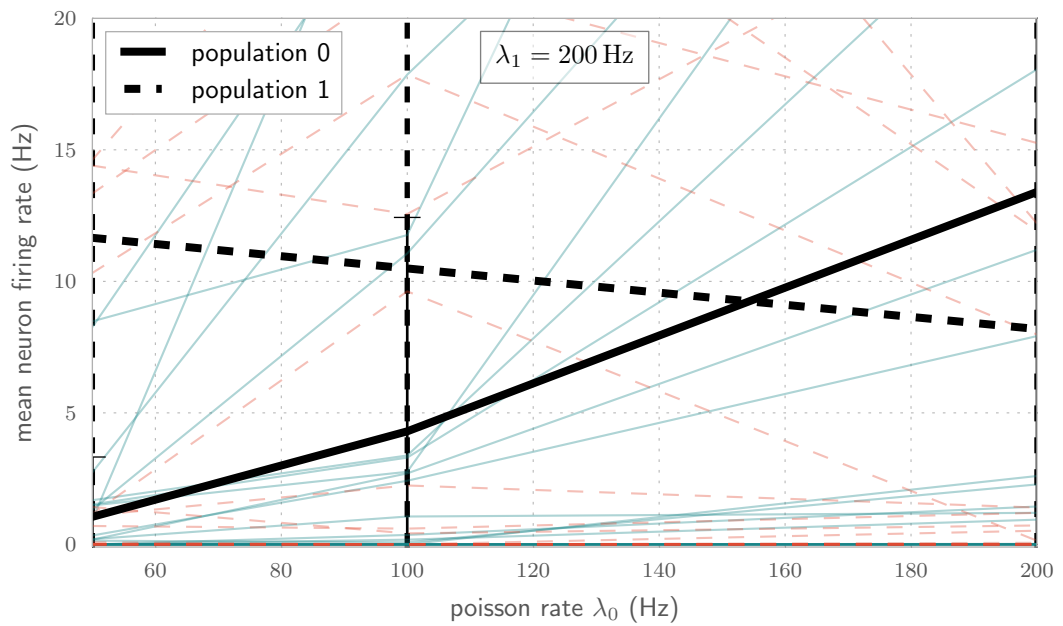
(b) Results from hardware measurement

Figure 3.6: The entire network is emulated with all connections as shown in figure 3.1. Population 1 receives constant poisson stimulus with rate  $\lambda_1 = 50$  Hz. Population 0 receives a poisson stimulus of different rate  $\lambda_0$  for each measurement step. The faded lines in the background are the means of 15 repeated measurements for each single neuron. The thick lines indicate the means of all neurons of one populations, error bars indicate the neuron-to-neuron standard deviations. The solid lines belong to population 0 and the dashed lines to population 1. Figure (b) is a zoom in the relevant ranges. The full plot can be found in appendix B.

### 3 Emulating a recurrent neural network



(a) Results from ESS measurement



(b) Results from hardware measurement

Figure 3.7: The entire network is emulated with all connections as shown in figure 3.1. The experimental setup is the same as described in figure 3.6 but with population 1 receiving a poisson stimulus of rate  $\lambda_1 = 200$  Hz. Figure (b) is a zoom in the relevant ranges. The full plot can be found in appendix B.

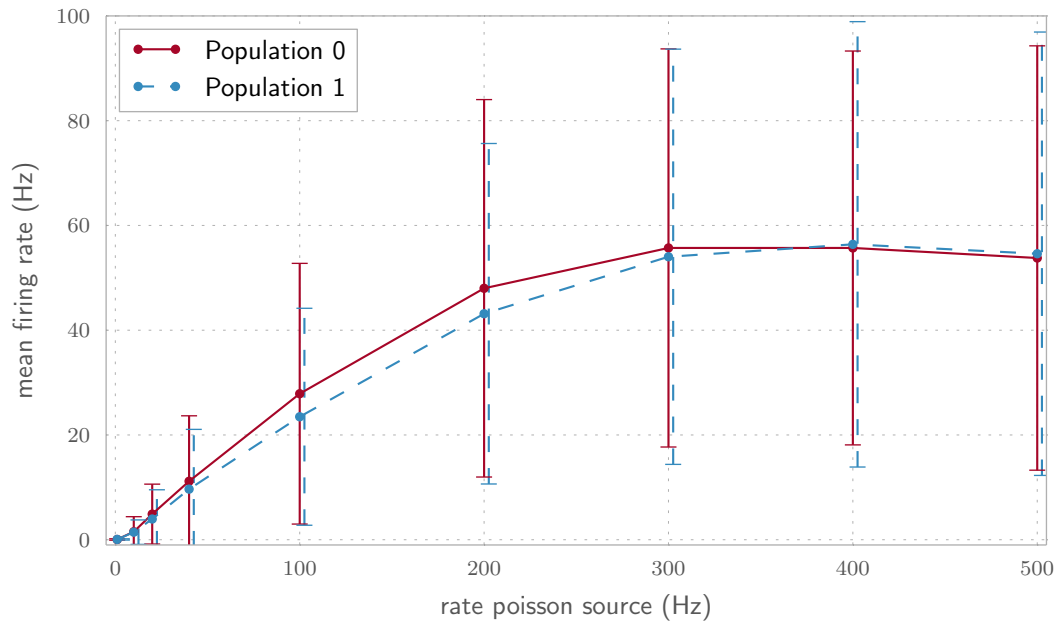
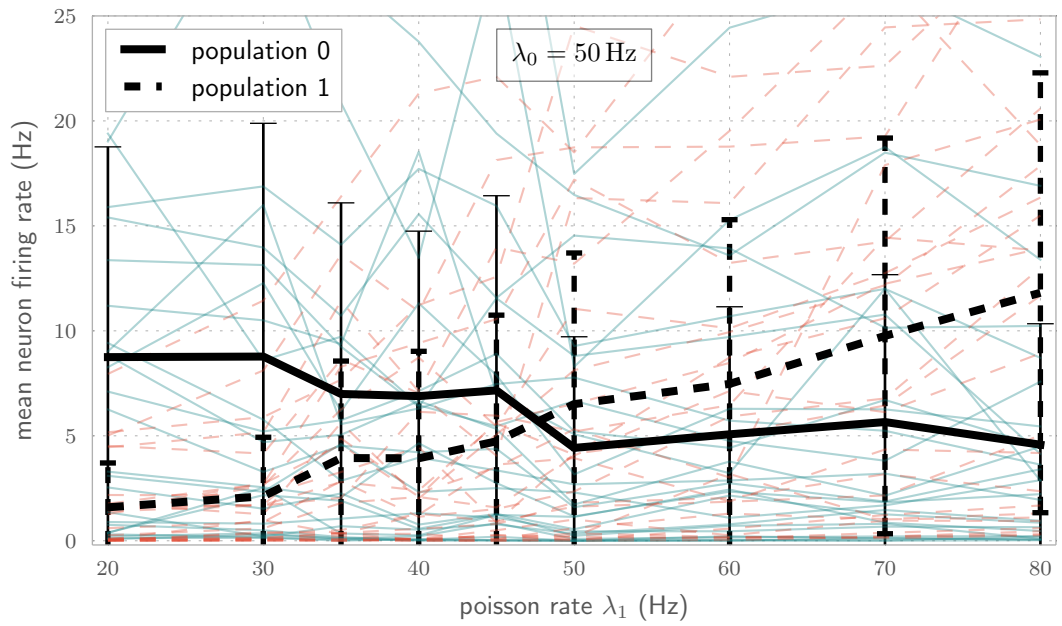
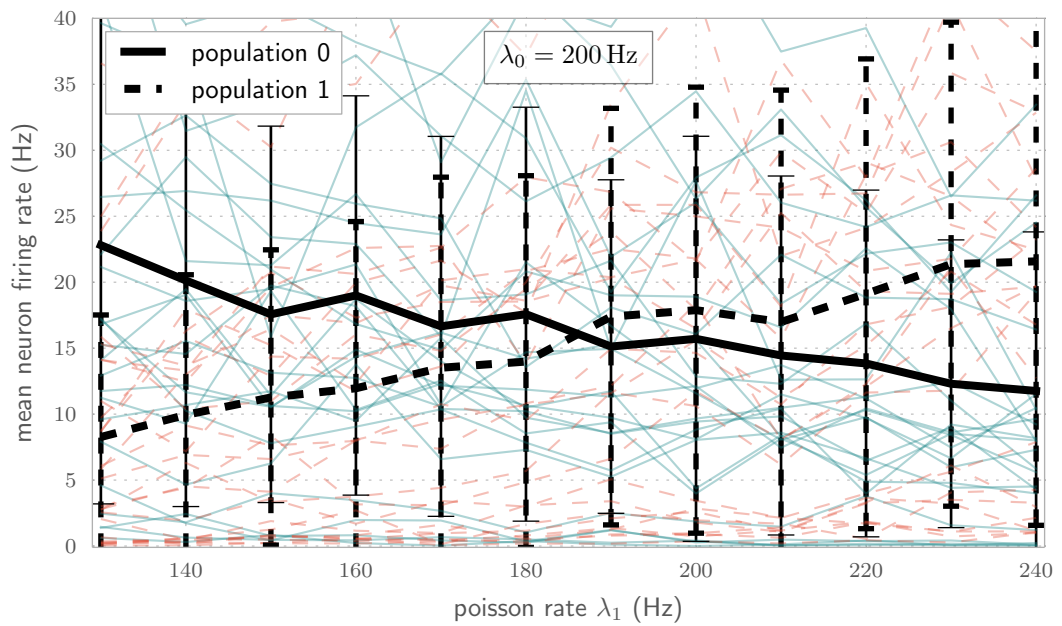


Figure 3.8: Each population is emulated independently, receiving different poisson stimulus. This is the same plot as shown in figure 3.3 but with correctly applied blacklisting. The plotted data points are the means of all 26 neurons which are determined as the means of 15 repeated measurements. The error bars indicate the standard deviations across the 26 neurons.

### 3 Emulating a recurrent neural network

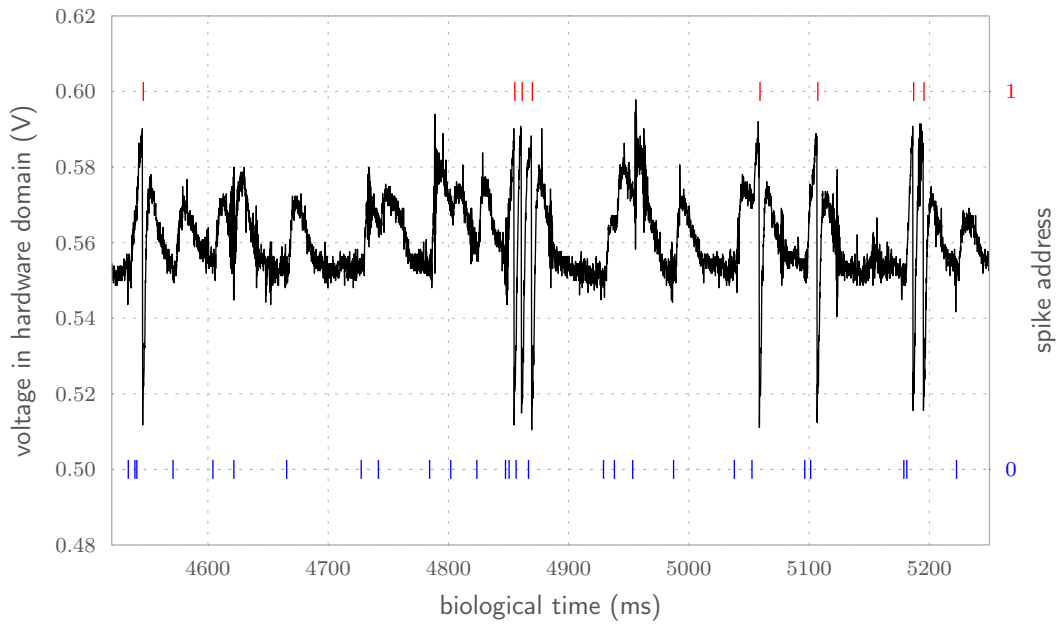


(a)

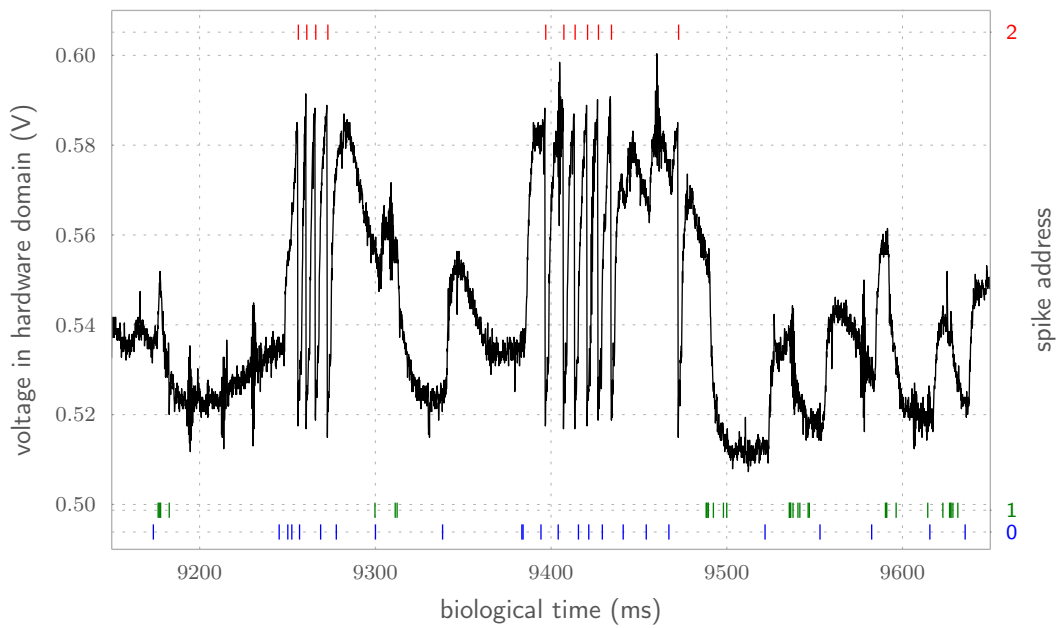


(b)

Figure 3.9: The entire network is emulated with all connections shown in figure 3.1. The same measurement setup as before is repeated but with correctly applied blacklisting. In this measurement the stimulus of population 1 is constant and the stimulus of population 0 is varied. The data points indicate the means across all neurons in one population which are determined by 15 repeated measurements. The error bars indicate the neuron-to-neuron standard deviations.



(a) Neuron without inhibition



(b) Neuron with inhibition

Figure 3.10: Voltage traces from an exemplary neuron in the network, emulated on hardware. In figure (a) only one population with external stimulus is emulated. The neuron does not have incoming inhibitory connections. Spike address 0 are the spike times of the poisson source and address 1 are the recorded spike events of the neuron. In figure (b) the entire network is emulated. The spike address 0 are excitatory stimulus events, spike address 1 are inhibitory events from the other population and spike address 2 are the recorded spike events of the neuron.

### 3 Emulating a recurrent neural network

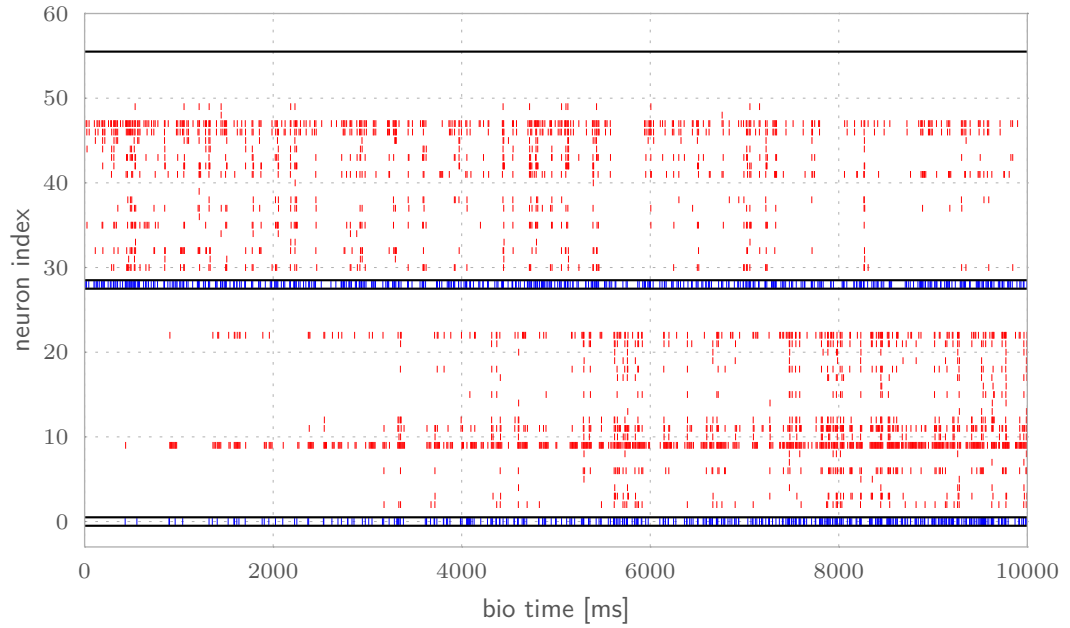


Figure 3.11: Raster plot for all neurons in the network for a single experiment run. The external stimulus of population 1 has a constant poisson rate of  $\lambda_1 = 50$  Hz. The rate of the external stimulus of population 0 is constantly increased in the range of  $1 \text{ Hz} \leq \lambda_0 \leq 300 \text{ Hz}$ ,  $\lambda_1 = 50$  Hz. Neuron index 0 and 28 are the spikes event of the poisson sources 0 and 1, respectively. Indices 2-27 are the neurons of population 0, indices 30-35 are the neurons of population 1.

## 4 Discussion and Outlook

In this thesis, a recurrent soft Winner Take All (sWTA) like neural network was implemented on neuromorphic hardware and investigated for its competitive dynamics. For conducting emulation experiments, the PyNN frontend was used giving access to the complex hardware structures through an easy to use high level frontend. Before investigating network dynamics, the hardware was characterized for parameter control from the PyNN interface. Those parameters available to the PyNN user after calibrating the hardware were investigated in their dynamic ranges. To have reliably spiking hardware neurons, a blacklisting measurement was implemented.

Finally, the sWTA like neural network was build up step by step in PyNN. The investigated network properties were developed using the Executable System Specification (ESS) as reference. Qualitatively similar results could be obtained in ESS simulation and hardware emulation. The major difference lies in overall spiking rates which are in simulation higher by a factor of 2 to 5, depending on the stimulus strength. Causes for differences can be found in missing or insufficient calibration, which is in a preliminary stage. Further, the hardware used for implementing the network is a prototype system still in development.

All in all it was possible to implement the neural network on a single HICANN chip, but there is room for improvement. The main focus in this thesis was on the implementation of the network and less on the investigation of network properties. Neuron spiking rates were averaged over several independent measurements. This does not take the possibly changing network dynamics into account. A possible solution would be to emulate the network with different stimulus rates within one experiment, avoiding the dependence of network dynamics on trial to trial variations.

All neurons of one population in the investigated network received always stimulus from the same external source. The resulting parallel activity and firing has strong influence in network dynamics, giving the first firing population advantage over the other one. To properly investigate network dynamics, neurons would need to receive individual stimulus. In single HICANN usage this would be strictly limited through bandwidth limitations. The next step would be to use several HICANNs, making it possible to emulate a greater number of neurons. This would also allow to choose only optimally behaving neurons and still be able to average over a large number. Another possible technique would be to investigate parameter noise in simulations with the ESS, e.g. by varying the parameters of the PyNN import.

This year the next version of the hardware chip, the HICANNv4, will be available for experiments. Hardware bugs will be fixed which limit parameter usage or put constraints on calibration possibilities. Additionally an implementation of a multi wafer scale system is planned which will make experiments over several wafer modules possible.

#### 4 Discussion and Outlook

With further developed and newly implemented calibration techniques, as well as further developed hardware specifications, more complex networks can be investigated for possible implementations. A network having already been investigated for theoretical implementation on the HICANN wafer system is the Cortical Layer 2/3 Attractor Memory network (*Petrovici et al.*, 2014). Even though the network is scalable in size, for a reasonable implementation the usage of multiple HICANNs is necessary. One reason is the high connectivity in the network, reaching limitations for single HICANN usage. Further, the network requires Short Term Plasticity (STP) and adaption mechanisms which have been characterized recently and will soon be available in the calibration work flow. One main method used for compensation for distortion mechanisms on the hardware was adapting the synaptic weights. Currently there is no detailed characterization and calibration of the synaptic weights available in the calibration work flow. Still, the basic requirements are fulfilled and a first approach on implementing a larger and more complex neural network on multiple HICANNs could be taken.



# Appendix

## A: Emulation Parameters

Parameter	Value
$C_m$	fixed calibration value
$\tau_m$	fixed calibration value
$\tau_{\text{refrac}}$	100 DAC ( $I_{\text{pl}}$ )
$\tau_{\text{syn,E}}$	fixed calibration value
$\tau_{\text{syn,I}}$	fixed calibration value
$E_{\text{rev,I}}$	-60 mV
$E_{\text{rev,E}}$	-40 mV
$V_{\text{reset}}$	-55 mV
$V_{\text{rest}}$	-50 mV
$V_{\text{thresh}}$	-47 mV
<i>weight</i>	4 nA

Table .1: Parameters used in PyNN. Neuron model used: IF\_cond\_exp

## B: Full sized emulation plots of sWTA network

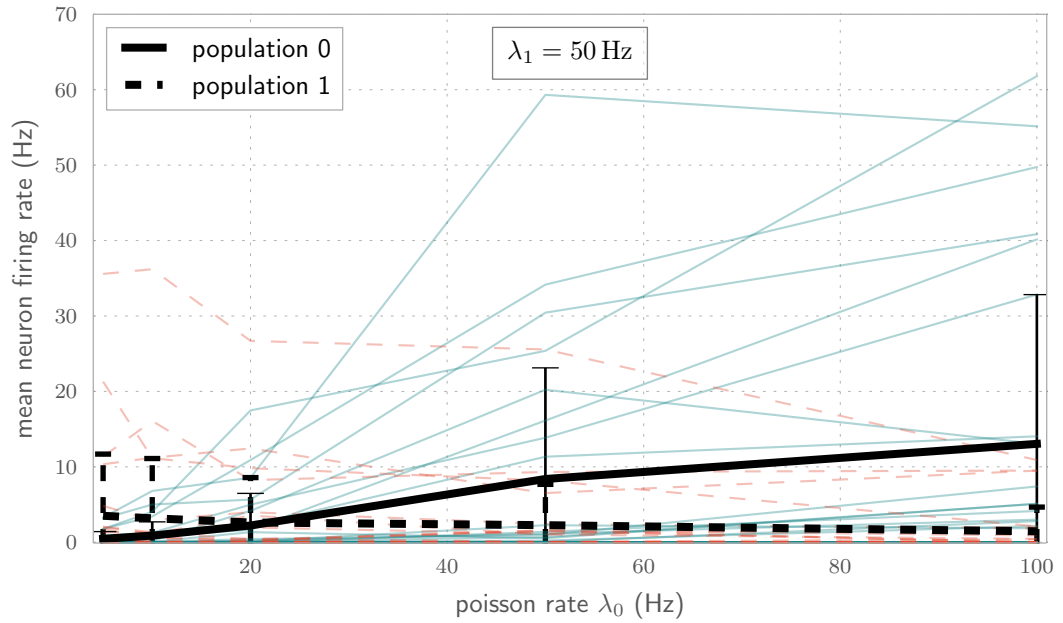


Figure 1: The full plot to 3.4b. Two populations are emulated but only population 1 receives inhibitory input from the population 0 as shown in figure 3.2b. The network is emulated for different population 0 stimuli  $\lambda_0$ . The poisson stimulus for population 1 is constant at  $\lambda_1 = 50$  Hz. The faded lines in the background are the means of 15 repeated measurements for each single neuron. The thick lines indicate the means of all neurons of one populations, error bars indicate the neuron-to-neuron standard deviations. The solid lines belong to population 0 and the dashed lines to population 1.

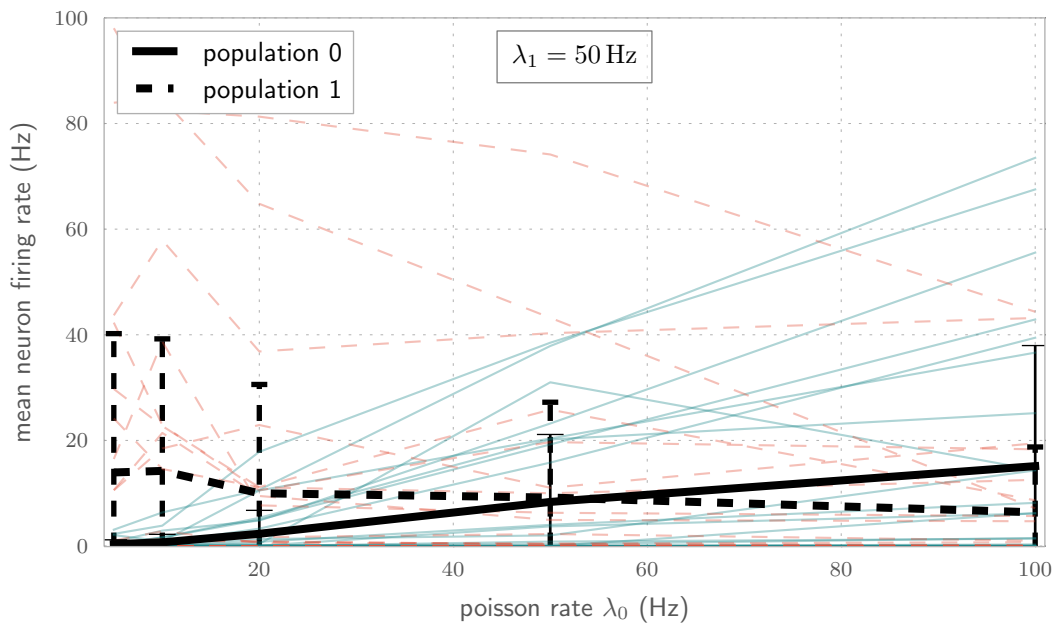


Figure .2: The full plot to 3.5b. Two populations are emulated but only population 1 receives inhibitory input from the population 0 as shown in figure 3.2b. The experimental setup is the same as described in figure .1 but with population 1 receiving a poisson stimulus of rate  $\lambda_1 = 200$  Hz.

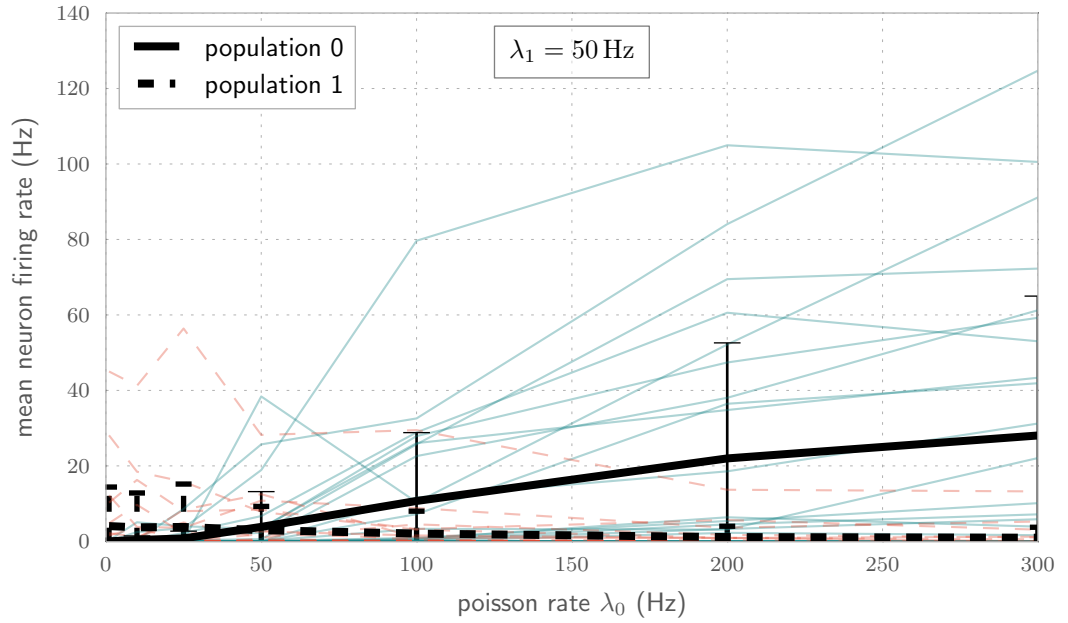


Figure .3: The full plot to 3.6b. The entire network is emulated with all connections as shown in figure 3.1. Population 1 receives constant poisson stimulus with rate  $\lambda_1 = 50$  Hz. Population 0 receives a poisson stimulus of different rate  $\lambda_0$  for each measurement step. The faded lines in the background are the means of 15 repeated measurements for each single neuron. The thick lines indicate the means of all neurons of one populations, error bars indicate the neuron-to-neuron standard deviations. The solid lines belong to population 0 and the dashed lines to population 1.

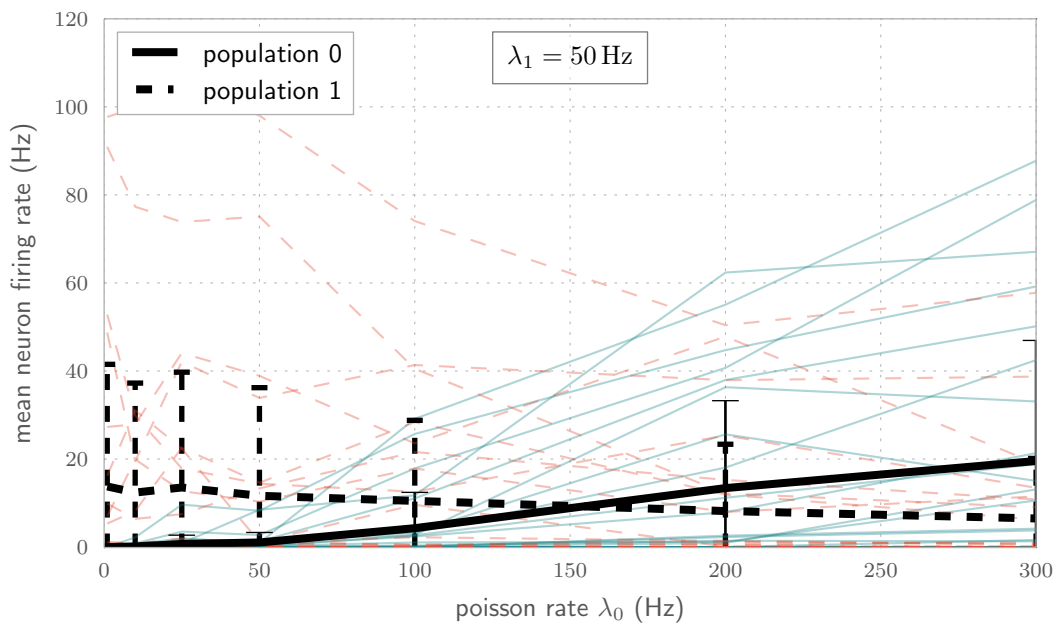


Figure .4: The full plot to 3.7b. The entire network is emulated with all connections as shown in figure 3.1. The experimental setup is the same as described in figure .3 but with population 1 receiving a poisson stimulus of rate  $\lambda_1 = 200$  Hz.



# List of Abbreviations

ESS .....	Executable System Specification
HICANN.....	High Input Count Analog Neural Network
AdEx .....	Adaptive Exponential Integrate and Fire
LIF .....	Leaky Integrate and Fire
sWTA.....	soft Winner Take All
STP.....	Short Term Plasticity
STDP.....	Spike-Timing Dependent Plasticity
PSP.....	postsynaptic potential
OTA .....	operational transconductance amplifier
DAC.....	digital to analog converted
DenMem .....	dendritic membrane circuit
DNC.....	digital network chip
FPGA .....	field programmable gate array
ISI .....	inter spike interval





# Bibliography

- Alevi, D., Investigation of a simple feed-forward neuronal network on neuromorphic hardware, *Internship rep.*, 2014, [Online]. Available: [http://www.kip.uni-heidelberg.de/cms/fileadmin/groups/vision/Downloads/Internship\\_Reports/report\\_alevi.pdf](http://www.kip.uni-heidelberg.de/cms/fileadmin/groups/vision/Downloads/Internship_Reports/report_alevi.pdf).
- Billaudelle, S., Characterisation and calibration of short term plasticity on a neuromorphic hardware chip, Bachelor thesis, University of Heidelberg, HD-KIP 14-93, 2014.
- Brette, R., and W. Gerstner, Adaptive exponential integrate-and-fire model as an effective description of neuronal activity, *J. Neurophysiol.*, *94*, 3637 – 3642, doi:NA, 2005.
- Cutsuridis, V., Bradykinesia models of parkinson’s disease, *Scholarpedia*, *8*(9), 30,937, doi:10.4249/scholarpedia.30937, 2013.
- Friedrich, A., Charakterisierung von adaption auf neuromorpher hardware, Bachelor thesis, University of Heidelberg, HD-KIP 15-10, 2015.
- HBP SP9 partners, *Neuromorphic Platform Specification*, Human Brain Project, 2014.
- Kiene, G., Evaluating the synaptic input of a neuromorphic circuit, Bachelor thesis, Universität Heidelberg, 2014.
- Müller, E. C., Novel operation modes of accelerated neuromorphic hardware, Ph.D. thesis, Heidelberg, Univ., Diss, 2014.
- Petrovici, M. A., et al., Characterization and compensation of network-level anomalies in mixed-signal neuromorphic modeling platforms, *PLOS ONE*, doi:dx.doi.org/10.1371/journal.pone.0108590, 2014.
- Pfeil, T., et al., Six networks on a universal neuromorphic computing substrate, *Frontiers in Neuroscience*, *7*, 11, doi:10.3389/fnins.2013.00011, 2013.
- Schemmel, J., D. Brüderle, A. Grübl, M. Hock, K. Meier, and S. Millner, A wafer-scale neuromorphic hardware system for large-scale neural modeling, in *Proceedings of the 2010 IEEE International Symposium on Circuits and Systems (ISCAS)*, pp. 1947–1950, 2010.
- Schmidt, D., Automated characterization of a wafer-scale neuromorphic hardware system, Masterarbeit, Universität Heidelberg, 2014.



## Statement of Originality (Erklärung):

I certify that this thesis, and the research to which it refers, are the product of my own work. Any ideas or quotations from the work of other people, published or otherwise, are fully acknowledged in accordance with the standard referencing practices of the discipline.

Ich versichere, dass ich diese Arbeit selbständig verfasst und keine anderen als die angegebenen Quellen und Hilfsmittel benutzt habe.

Heidelberg, March 20, 2015

.....  
(signature)